Università degli Studi di Padova

Dipartimento di Fisica e Astronomia
Corso di Laurea in Fisica

Equilibrium and dynamical properties of polymer chains translocating through a rigid membrane

Laureando:
Daniele Schiavi

Relatore:
Prof. Enzo Orlandini
Corelatori:
Prof. Marco Baiesi

Anno accademico 2015/2016

Contents

List of Figures

Introduction

Polymers provide a variety of problems in science, they are subject of study for different discipline, like chemistry, biology and physics. They constitute a lot of synthetic object of which we have also experience (like plastics) and also biological matter (DNA, RNA and various other biological macromolecules are polymers).
While every discipline have their own approach to polymers, physics focus on studying them in a scale length very large where the microscopic details are negligible. At this scale the tools given by classical statistical mechanics are fundamental to study the configurational properties of polymer networks.

The behaviour of polymers is studied with different models and also depends on the space in which they are located.
Models where the polymer is embedded on a lattice are based on simple descriptions of polymers, for example in terms of random walks. Thanks to these oversimplified models was possible to exact results relative to thermodynamics properties.
More refined and realistic models have to take into account the excluded volume effect, due to the impenetrability of the atoms; the effect in a lattice is well reproduced by SAWs (self avoiding walks). The importance of excluded volume became more clear, in fact the study of critical phenomena gives a connection between SAWs and critical magnetic systems. There is a correspondence between the partition function of SAWs and the correlation function of a $O(n)$ model, that is a n-components, spin model, in the limit of $n \to 0$.

This correspondence allow us to use the known renormalization techniques, developed for systems near the criticality. The idea behind the renormalization group theory is that in a coarse grained model, as the scale becomes

larger the system (that is self similar) is less influenced by the microscopic details and universal properties start arising.

The concept of universality becomes also relevant for polymers, whose behaviour at scales much than the monomer size is not affected by the chemical details. Different systems follows the same universal scaling laws and belong to the same universality class, with the same critical exponents.
The study of discrete models is easier from an analytical and computational point of view and the results obtained obey the same scaling laws as the continuum models, with the same critical exponents. In fact the SAWs on a lattice and polymers in a good solvents belongs to the same universality class.

In this thesis we investigate a problem quite important in polymer science, namely the translocation of polymer through a membrane: the understanding of this dynamic is fundamental to many biological system, such as RNA translocation across nuclear pores, protein transport through membrane channels, transfer of genetic material from virus to an host cell and so on. The mechanisms of polymer translocation are many and different: it seems that there is not a single universal mechanism driving the phenomenon. Each case studied in literature treats different kind of translocation, like in case of charged polymer in where in the two halves of the space we have an electric potential difference, or in the case of there is a wall that is attractive from one side and repulsive from the other.

In our work we focus on the importance of topological constraint in translocation. Previous studies suggest that the dynamic of translocation is affected both by the presence of knots along the polymer backbone and by anchoring of a polymer end to the surface. The importance of studying this case arise from the various topological configuration that a polymer could have, in fact for very large polymers it has been shown that knots are usually present.
The experimental progress in the field and the non universality of the process make necessary to investigate further which factors determine the behaviour of the polymers during translocation.

In this thesis we use an off lattice model (a bead spring model) in which the polymer is a series of atoms, each connected to the next one with a potential that near the typical length of the bond is similar to an harmonic one.
It is fundamental to consider the excluded volume, so that the dynamic preserves the topology.
One of the main goal we want to achieve is an estimate of the free energy landscape of a polymer during an ubiased translocation.

This work is divided in two parts: in the first part we present an overview c of the theory behind the physics of polymer, we discuss models of polymers, focusing on the properties and characteristics of SAWs, then we see the correspondence between them and the magnetic system, finally we study the importance of knots in the dynamics of polymers. In the second part we present the techniques of simulation, and finally in Chapter 5 we present about the the numerical results and the estimate of the free energy and the entropic exponents for translocating polymers with different topologies.

Chapter 1

Polymer theory

A polymer is a molecule, or a macromolecule, composed of a several number of repeated subunits, these fundamental subunits are called monomers. The polymer can be seen as long concatenation of segments with a length negligible respects to the polymer's length. The dynamic is determined by the interaction between the solvent and monomers and the interaction between monomers.

Polymeric systems are usually too complicated to treat: the various degrees of freedom of the molecule make it difficult to study and obtain exact results. Since they are complex systems it becomes useful using the tools of mechanical statistics, which allows developing a statistical theory of the polymer.

Similar to gases for which we have quantity like the pressure, we can define some macroscopic quantity characterizing the system; for the polymers these quantities are, for example, the end-to-end distance or the gyration radius. The first one is defined as

$$\boldsymbol{R}_{ee} = \sum_{i}^{N} \boldsymbol{R}_i \tag{1.1}$$

where $\boldsymbol{R}_i$ is the position of the i-th monomer. This quantity has little physical meaning, in fact it depends only from the first and the last monomer, and, instead of it, it is preferred its square, that is needed to define the gyration radius:

$$\boldsymbol{R}_g^2 = \frac{1}{N} \sum_{i=1}^{N} (\boldsymbol{R}_i - \boldsymbol{R}_{ee})^2 \tag{1.2}$$

The average of this quantity is expected to follow the scaling law:

$$\langle R_g^2 \rangle \sim N^{2\nu} \tag{1.3}$$

the ν is called metric exponent and, for homopolymers, it relates to the fractal dimension of the system $D = 1/\nu$.
The metric exponent depends strongly on the interaction between solution and the polymers and the dimension of the space where the chain is embedded. For real polymers in a dilute "good" solution (the attraction between monomers and solvent is stronger than the monomer-monomer one) the exponent is $\nu \simeq 3/5$.

1.1 Discrete polymers model

Let the system be in a dilute solution and consider the case of a linear flexible chain. Each configuration of the chain in the space can be specified by the coordinates of the components. We denote, for a chain of $N+1$ elements, the coordinates of the j element as $\boldsymbol{R}_j$, where $j = 0, \ldots, N$. Since the statistical properties depends only on the relative position of the monomers, we can translate the polymer so that the 0-th element coincides with the origin.

In general, the partition function for the system can be written as

$$Z = \int \exp\left[-\beta U(\{\boldsymbol{R}_N\})\right] \mathrm{d}\{\boldsymbol{R}_N\}, \tag{1.4}$$

where $\{\boldsymbol{R}_N\} = \{\boldsymbol{R}_j\}_{j\in\{0,\ldots,n\}}$ is the set of coordinates and U is the total potential energy; it may be expressed as

$$U(\{\boldsymbol{R}_N\}) = \sum_{j=1}^{n} u_j(\boldsymbol{R}_{j-1}, \boldsymbol{R}_j) + W(\{\boldsymbol{R}_N\}). \tag{1.5}$$

The potential u_j takes in account that the $j-1$th e jth elements are connected through a bond, while the potential W includes all other interaction, like bond angle restriction, long range interaction, etc.; in (1.5) we have already integrated over the coordinates of the solvent molecules and W is a potential of a mean force. Using $\boldsymbol{r}_j = \boldsymbol{R}_j - \boldsymbol{R}_{j-1}$, called bond vector, we define a distribution:

$$\tau_j(\boldsymbol{r}_j) = \exp\left[-\beta u_j(\boldsymbol{r}_j)\right], \tag{1.6}$$

with the following normalization:

$$\int \tau_j(\boldsymbol{r}_j)\mathrm{d}\boldsymbol{r}_j = 1, \tag{1.7}$$

which sets the zero of the potential; furthermore the system is supposed to be homogeneous in space. The latter distribution is often referred as the bond distribution, since it is the length distribution of the bonds.

If we suppose $u_j(\boldsymbol{r}_j)$ to be spherical symmetric, the (1.4) can be rewritten as

$$Z = \int \left[\prod \tau_j(r_j)\right] \exp\left(-\beta W(\{\boldsymbol{r}_j\})\right) \mathrm{d}\{\boldsymbol{r}_j\} \tag{1.8}$$

Now, if the first element is fixed at the origin, the end-to-end distance $\boldsymbol{R} = \boldsymbol{R}_n$ is obtained integrating the distribution over the relative position under the following constraint,

$$\sum_{j=1}^{n} \boldsymbol{r}_j = \boldsymbol{R}. \tag{1.9}$$

This quantity is not very useful, it tells very little about the polymer, in fact it depends only on the positions of the first and last element.

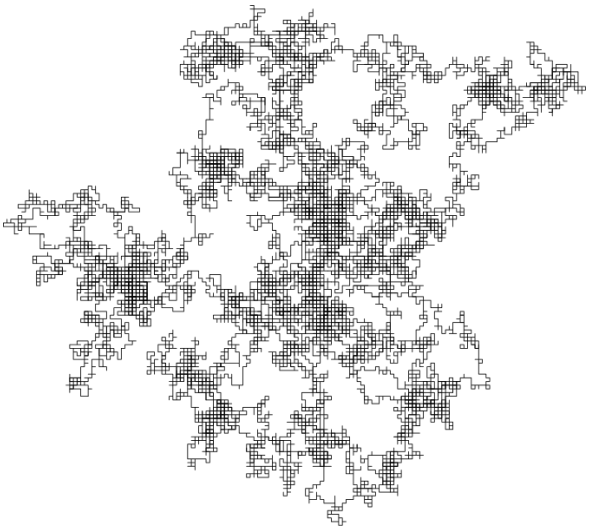

(a) A random walk on a square lattice of 25000 steps

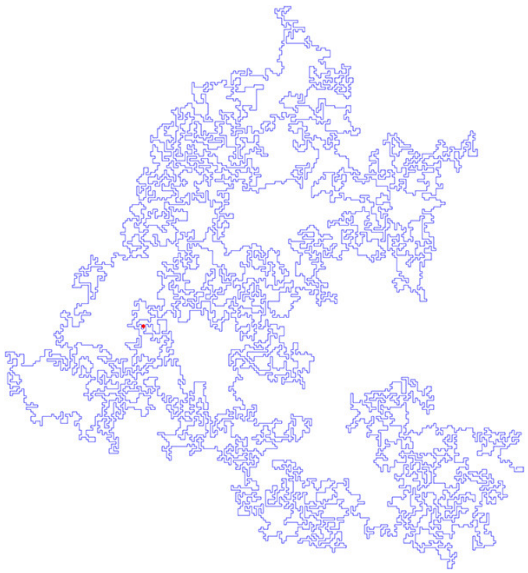

(b) A self avoiding walk on a square lattice of 11000 steps

Figure 1.1: In this figure we compare two dimensional discrete models in (a) there is a random walk $\nu = 1/2$ in (b) a self avoiding walk $\nu = 3/4$

1.1.1 Random walk

In this instance the polymer is described as a set of vertices or as a set of bonds in a lattice. The choice of the lattice is fundamental: the statistical properties, as we will see, depends on the topology of the space in which the chain is embedded.

One of the simplest model of polymer in discrete space is the random walk on a lattice.
A random walk is a stochastic process in which at each step you can go to one of the nearest site with the same probability; the sites (in this case they will be the vertices of the lattice) that you have been visited will derfine the polymer. For random walks it is possible to have exact results: we present some of them for an hypercubic lattice $\mathbb{Z}^d$.

The enumeration of the possible walks with N-steps

$$c_N = 2^d \tag{1.10}$$

Knowing that in a random walk each step is independent, it's easy to prove that:

$$\langle R_g^2 \rangle = \sum_{i,j \in \omega_N} \delta_{ij} = N \tag{1.11}$$

where ω_N is a set of N points in the lattice.
This result does not depends from the dimension of the lattice, so we can conclude, using (1.3), that the metric exponent $\nu = 1/2$.
It's useful to calculate also the number of the random walks that in an even number of step N return to the starting point, in one dimension:

$$q_N = \binom{N}{N/2} \tag{1.12}$$

For very large N and using the Stirling formula we obtain the following asymptotic behaviour:

$$q_N \simeq 2^N N^{-1/2} \tag{1.13}$$

This result can be generalized to more dimension.
We obtain the value of the entropic exponents for random walk, in fact considering the following scaling laws for polymer models:

$$c_N \simeq \mu^N N^{\gamma-1} \tag{1.14}$$

$$q_N \simeq \mu^N N^{\alpha-2} \tag{1.15}$$

where μ is the coordination number of the lattice. The exponents for the random walk are $\gamma = 1$ and $\alpha = 2 - d/2$ and since are universal quantity they have the same value for every lattice.

Random walks are not a good model for real chains, they only fits ideal chains; in fact we are neglecting the excluded volume effect, using a random walk the polymer is allowed to visit a site more than once.
Although these problems, they are a correct model for polymers in $d \geq 4$ or for polymer below the θ-point in $d \geq 3$ (which describes a polymer in poor solvent in which it tends to collapse).

1.1.2 Self avoiding walks

Due to the impenetrability of the atoms random walks fails giving a description for real chains; self-avoiding random walks (SAWs) describes linear chain in which the self-avoiding constrain represents the excluded-volume effect.
A SAW is still a random walk embedded in a particular lattice. In this case the calculation are more realistics and it can approximate quite well the behaviour of real polymers.

A SAW is a path which doesn't visit the same site (or bond if we are talking about bond animal) twice or more. Let consider a $\mathbb{Z}^d$ lattice, the partition function for an N-step SAW is given by:

$$Z_n = \sum_{\omega \in \Omega_n} 1 \tag{1.16}$$

The partition function is the sum over each configuration $\omega = \{\boldsymbol{r}_0, \ldots, \boldsymbol{r}_n\}$ in the ensemble Ω_n with the same weigh.

Counting the number of SAWS

In order to calculate the partition function we have to consider the total number of self avoiding path on a given lattice; the situation is quite different from the case of random walks where we have exact results. However we can estimate the asymptotic behaviour for large N and exact numerical results for small N. In the following results we don't count the paths that can be translated onto the other.'

Let C_N be the number of possible SAWs with N steps, we can easily give some bounds to this quantity. In fact we know for sure that the SAWs must be lower than the total random walk and greater than the directed walks (which are path on lattice that can make only non-negative steps).
After these considerations and if we're working on a hypercubic lattice, we get the following inequalities for SAWs:

$$d^N \leq c_N \leq (2d)^N. \tag{1.17}$$

Other important inequality is:

$$c_{M+N} \leq c_N c_m \tag{1.18}$$

or

$$\log c_{M+N} \leq \log c_N + \log c_m \tag{1.19}$$

Every $N+M$-SAW can be obtained attaching an N-step SAW to an M-step SAW, while generic path obtained by joining two generic SAWs might not be a SAW. The logarithm of the number of SAW is subadditive, property that follows from (1.19).
Thanks to this property of $\log c_{N+M}$ and Fekete's lemma it can be proved that the following limit exists (see[17]):

$$\lim_{N\to\infty} \frac{1}{N} \log c_N = \mu. \tag{1.20}$$

where μ is the connective constant.

In the limit for $n \to \infty$ it is proven that the number of SAP (self avoiding polygon), which are whose $(N-1)$-th step is a nearest-neighbor of the starting point, is the same of SAWs.
Let q_n the number of SAPs of length N, we can give a concatenation rule as (1.18):

$$q_{N+M} \geq \frac{q_N q_M}{d-1} \tag{1.21}$$

The result above is sufficient to prove the existence of the following limit:

$$\lim_{N\to\infty} \frac{1}{N} \log q_N = \mu \tag{1.22}$$

where, as we said before, the connective constant is the same of the one in (1.20).

While the connective constant depends on the choice of the lattice, therefore isn't a universal, it still is an important quantity that appears in universal

laws. The calculation of the connective constant is quite difficult and mostly are numerical results, there are few exact results (like for the hexagonal lattice).
We will see that, despite the lattice dependence, its value will not change if we add some geometric constraint.

1.1.3 SAWs interacting with a wall

We now focus on of the behaviour of a polymer in presence of a surface; in this case we have to add a constraint: that one or more vertices are joint to a surface and we are going to see that, in case the chain is not adsorbed, the connective constant is equal to the polymer free in the bulk.

Let consider the problem of a polymer (we consider it embedding in a hypercubic lattice) attached to a surface ($x = 0$) restrained to remain in one of the half-spaces; we define as c_N^1 the number of N-step SAWs with the starting point fixed at $x_0 = 0$ and c_N^{11} the number of N-step SAWs with both terminal vertices fixed such that $x_0 = x_N = 0$.
We shall show that the limits for c_N^1 and c_N^{11} corresponding to (1.20) and have the same value. Let consider the polygon embedding in the bulk lattice, without loss of generality, we can consider the one with starting and ending point on the surface $x_0 = x_N = 0$. Therefore we obtain the following result:

$$q_N \leq c_N^{11} \leq c_N^1 \leq c_N \tag{1.23}$$

and using the squeeze theorem and the equations (1.20) and (1.22) we have:

$$\lim_{N\to\infty} \frac{1}{N} \log c_N^{11} = \lim_{N\to\infty} \frac{1}{N} \log c_N^1 = \mu \tag{1.24}$$

The connective constant is the same one for a free polymer in bulk, the dominant term in the asymptotic behaviour neglects the presence of a wall. However, even if they have the same dominant term, we will see that the cases treated above (c_N,c_N^1,c_N^{11}) have a different subdominant behaviour and, in fact, they have different entropic exponents.

1.2 Continuos polymer model

In this section we treat models outside lattice, these models come handy when we use renormalization group calculations for polymers, which are more precise in the continuum. We start with a model similar to the one for the

random walk and then we will see what happens when we consider the self avoiding effect.

1.2.1 Brownian chain

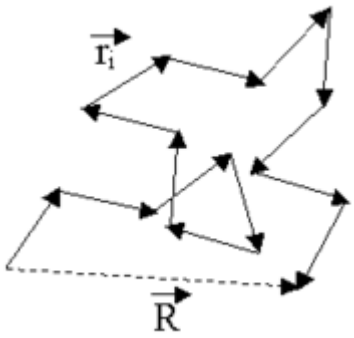

Figure 1.2: An example of ideal chain

A similar model to the random walk is the Brownian chain. We consider the segments of the chain have a mean length l finite and the probability associated to each segment of the polymer $\boldsymbol{r}_i$ (where $i = 1, \ldots, N$) independent from the position of the others segment, isotropic and identical.
It satisfies the following property:

$$\langle \boldsymbol{r}_i \cdot \boldsymbol{r}_j \rangle = \delta_{ij} l^2 d \tag{1.25}$$

where the mean is taken respect to the probability $p(\boldsymbol{r})$.
In order to calculate the gyration radius is convenient to use the probability function of the end to end radius $p_N(\boldsymbol{R})$.

$$p_N(\boldsymbol{R}) = \int \delta(\boldsymbol{R} - \boldsymbol{R}_{ee}) \prod_{i=1}^{N} dp(\boldsymbol{r}_i) \boldsymbol{r}_1 \ldots \mathrm{d}\boldsymbol{r}_N, \mathbb{R}^{Nd} \tag{1.26}$$

Knowing that $\boldsymbol{R}_{ee}$ depends only to the last and first element and performing the integral over the other $N - 1$ variables, we obtain that:

$$p_N(\boldsymbol{R}) = \langle \delta(\boldsymbol{R} - \boldsymbol{R}_{ee}) \rangle \tag{1.27}$$

Let $\tilde{p}_N(\boldsymbol{k})$ be the Fourier transform:

$$\tilde{p}_N(\boldsymbol{k}) = \langle e^{i\boldsymbol{k}\cdot\boldsymbol{R}_{ee}} \rangle = \langle e^{i\boldsymbol{k}\cdot\boldsymbol{r}} \rangle^N \tag{1.28}$$

When N is large, $\tilde{p}_N(k)$ is appreciable only for $k \simeq 0$, so we can expand the function in the neighbourhood of $k = 0$

$$\tilde{p}(\boldsymbol{k}) = 1 - \frac{k^2 l^2}{2} + \ldots \simeq e^{-Nk^2 l^2/2} \tag{1.29}$$

In order to obtain the expression for $p_N(\boldsymbol{R})$ we perform the Fourier anti transform:

$$p_N(\boldsymbol{R}) = \frac{1}{(2\pi N l^2)^{d/2}} e^{-\frac{R^2}{2Nl^2}} \tag{1.30}$$

This result is a merely an application of the central limit theorem, since $\boldsymbol{R} = \sum_{i=0}^{N} \boldsymbol{r}_i$ is the sum of random independent variables for large N.

The average gyration radius scales with the same law of the random walk:

$$\langle R_g^2 \rangle \sim N \tag{1.31}$$

Now we perform a limit in the continuum that gives as result the proper Brownian chain. Let $S = Nl^2$ (this quantity define the size of the Brownian chain), the limit is performed reducing $l \to 0$ and taking $N \to \infty$ such that S is finite.
As coordinates to locate a point on a curve one can be use $s = il^2$, where $i = 0, \ldots, N$, thus the position is parametrized by $\boldsymbol{r}(s)$. The parameter s has the dimension of an area, this is compatible to the fact that the Haussdorf dimensionality is 2 and, so, the Brownian chain has the characteristic of an area.

At any configuration of the chain we associate a Gaussian like weight:

$$W(\boldsymbol{r}_0, \ldots, \boldsymbol{r}_N) = e^{-\frac{1}{2l^2} \sum_{i=1}^{N} (\boldsymbol{r}_i - \boldsymbol{r}_{i-1})^2} \tag{1.32}$$

We use a weight to perform the limit and not a probability distribution, because there is not a limit for the latter due to the normalization constant. The positions, for $(i-1)l^2 \leq s \leq il^2$, obeys the following relations:

$$\begin{aligned} \boldsymbol{r}(s) &= \boldsymbol{r}_{i-1} + \left(\frac{s}{l^2} - i + 1 \right) (\boldsymbol{r}_i - \boldsymbol{r}_{i-1}) \\ \frac{d\boldsymbol{r}(s)}{ds} &= \frac{1}{l^2} (\boldsymbol{r}_i - \boldsymbol{r}_{i-1}) \end{aligned} \tag{1.33}$$

Therefore the statistical weight defined before can be written in the form:

$$W(\boldsymbol{r}(s)) = \exp\left(-\frac{1}{2} \int_0^S \left(\frac{d\boldsymbol{r}(s)}{ds} \right)^2 ds \right) \tag{1.34}$$

1.2.2 Edwards model

The previous model describes the ideal chain, the physics is the same of the random walk: they belong to the same universality class. In order to describe real chain we have to add a repulsive short range interaction, that reproduces the self avoiding effects.
We use the weight we have previously calculated adding a contact interaction:

$$W_N(\boldsymbol{r}(s)) = W_0(\boldsymbol{r}(s)) \exp\left(-\frac{b}{2}\int_0^S \int_0^S \delta(\boldsymbol{r}(s) - \boldsymbol{r}'(s'))\, ds\, ds'\right) \tag{1.35}$$

where W_0 is (1.34).
The parameter b is the strength of the interaction, if $b = 0$ we obtain the Brownian chain, this kind of weight punishes self encounters. Thus for $b \to \infty$ only self avoiding paths survive.

It is possible to perform a scale transformation in which $s = S\lambda$ and $\boldsymbol{x} = \sqrt{s}\boldsymbol{r}$. Using the Dirac delta property $\delta(ax) = \delta(x)/|a|$, the interaction term become:

$$\frac{b}{2} S^{2-d/2} \int_0^1 \int_0^1 \delta(\boldsymbol{x}(\lambda) - \boldsymbol{x}'(\lambda'))\, d\lambda\, d\lambda' \tag{1.36}$$

From this equation in dimension $d > 4$ for long chains $S \to \infty$ the interaction term vanishes and this is consistent to the fact that in these dimensions the Brownian chain is a good model for polymers.
We can absorb the terms outside the integral in a new coupling constant $z = (2\pi)^{-d/2} b S^{2-d/2}$ and the divergence appears in this term.

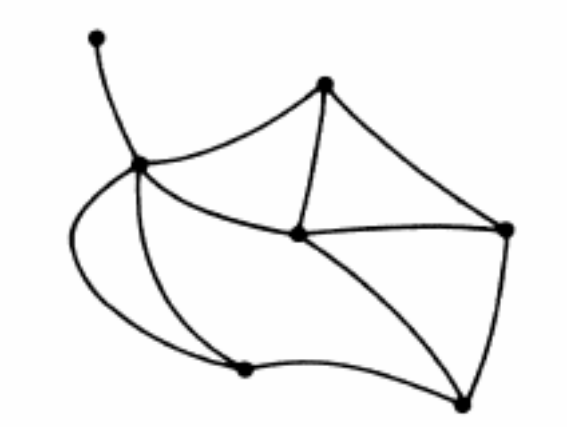

Figure 1.3: General polymer network with $\mathcal{N} = 11$ and with $\mathcal{L} = 5$ loops

1.3 Entropic exponent

We consider a polymer network with a general topology G, as the one depicted by Fig 1.3.
The partition function for the polymer network is:

$$Z(G) = \int d[\boldsymbol{r}]\; W_{\mathcal{N}}[\boldsymbol{r}]\delta(G)\left(\int W^0_{\mathcal{N}}[\boldsymbol{r}]\prod_{a=1}^{\mathcal{N}}\delta(\boldsymbol{r}_a(0))\,d[\boldsymbol{r}]\right)^{-1} \tag{1.37}$$

The $\delta(G)$ is a symbolic delta and represent the product of all δ necessary in order to obtain the topology (it connect the chains to their final vertices). The $W^0_{\mathcal{N}}$ is the weight of the Brownian chain of the network:

$$W^0_{\mathcal{N}}[\boldsymbol{r}] = \prod_{a=1}^{\mathcal{N}}\exp\left[-\frac{1}{2}\int_0^S\left(\frac{d\boldsymbol{r}_a}{ds}\right)^2 ds\right] \tag{1.38}$$

while the other weight is the one of the interacting system:

$$W_{\mathcal{N}}[\boldsymbol{r}] = W^0_{\mathcal{N}}[\boldsymbol{r}]\prod_{a,a'=1}^{\mathcal{N}}\exp\left[-\frac{b}{2}\int_0^S\int_0^S\delta(\boldsymbol{r}(s)-\boldsymbol{r}'(s'))\,ds\,ds'\right] \tag{1.39}$$

The number of topological constraint Δ i.e. number of $\delta(\boldsymbol{r})$ in $\delta(G)$:

$$\Delta = \sum_{L\geq 1}(L-1)n_L + 1 \tag{1.40}$$

where n_L is the number of vertices with L legs, e.g. in the figure 1.3 there are $n_1 = 1$, $n_3 = 4$,$n_4 = 1$ and $n_5 = 1$.

It can be shown the partition function, writing all dependencies:

$$Z(G, b, S, d) = S^{(\mathcal{N}-\Delta)d/2}\mathcal{Z}(G, z, d) \tag{1.41}$$

where $\mathcal{Z}$ is a dimensionless quantity that depends to z. For $z = 0$,i.e. in absence of self avoiding interaction, $\mathcal{Z}$ is constant and is obtained the entropic exponent for a polymer network made by Brownian chains:

$$\gamma_G - 1 \equiv -\mathcal{L}\frac{d}{2} = (\mathcal{N}-\Delta)\frac{d}{2} \tag{1.42}$$

Where $\mathcal{L}$ is the number the loops in the polymer network:

$$\begin{aligned}\mathcal{L} &= \sum_{L\geq 1}\frac{1}{2}(L-2)n_L + 1\\ 2\mathcal{N} &= \sum_{L\geq 1}Ln_L\end{aligned} \tag{1.43}$$

In the limit for $z \to \infty$ the dimensionless part of the partition function scales as:

$$\mathcal{Z}(G) \sim z^{\sigma_G/(2-d/2)} \sim S^{\sigma_G} \tag{1.44}$$

The quantity is diverging but can be renormalized, the diverging Brownian area S is substituted by the renormalized physical quantity that is the gyration radius.
Trough renormalization techniques we have new renormalized exponent $\hat{\sigma}_L$ are associated to the vertices and we obtain the hyperscaling relation:

$$\gamma_G - 1 = \sum_{L \geq 1} n_L \hat{\sigma}_L - \nu d \mathcal{L} \tag{1.45}$$

The $\hat{\sigma}_L$ in the excluded volume limit, calculated in $d = 4 - \epsilon$ expansion, is:

$$\hat{\sigma}_L = \frac{\epsilon}{16}(2 - L)L + O(\epsilon) \tag{1.46}$$

The $\hat{\sigma}$ have different possible values, depending on the geometry of the system: for example the one calculated for the bulk one is different from the one calculated for a polymer with final vertices onto a surface.

Chapter 2

Critical properties

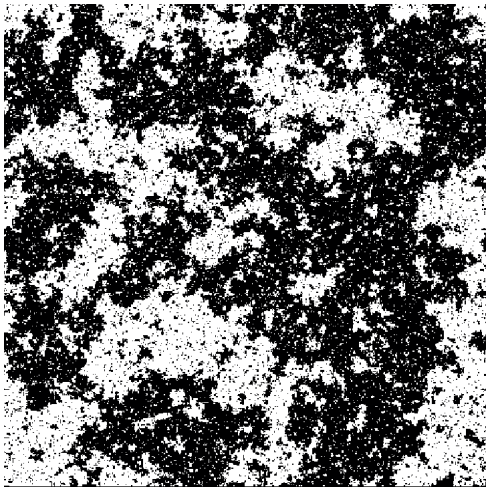

(a) A critical Ising system

(b) A self avoiding walk

Figure 2.1: These figures represent two critical systems, all this systema have the peculiarity of being scale invariant

In this chapter we focus on the strong relation between linear, flexible polymers with some features of critical phenomena, more precisely to a critic magnetic system.
For magnetic system the characterizing quantity is the magnetization M, that is a function of the temperature T and the field B. For $B = 0$ one can guess naively that the magnetization vanish under the symmetry of the system, in the Ising model one can think that there is the same chance that a site have spin up or down, this is true for high temperature.
There exists a critical temperature under which the free energy have a de-

generated minima and the system reach one of them and the magnetization have a finite value. Little above this temperature there are forming finite size domains (region with non zero average magnetization); the characteristic size ξ of this cluster follow a scale law:

$$\xi \simeq |\epsilon|^{-\nu} \quad (\epsilon \to 0) \tag{2.1}$$

where $\epsilon = T - T_c$. This length is called correlation length and near the criticality the systems forget the detail and tend to a universal regime. The structure have a strong analogy with the polymer in a good solution: looking the characteristic length of the polymer given by the gyration radius we notice a correspondence between N^{-1} and ϵ.
This analogy can be shown more rigorously and that proves this two systems lives in the same universality class.

2.1 Relation with critical phenomena

Following de Gennes [5] we can relate properties of real polymers (in this case the SAW model) to those of the $O(n)$-model in the formal limit $n \to 0$ near the critical point.

The $O(n)$-model is a spin model in which the symmetry of the spin is $O(n)$. This model is very known in physics, the $O(1)$ model is the Ising model, or $O(3)$ is the Heisemberg model.
Consider the following Hamiltonian, similar to the Ising's one in which we use a nearest neighbor interaction:

$$-\beta H = \sum_{\langle ij \rangle} K_{ij} \boldsymbol{s}_i \cdot \boldsymbol{s}_j. \tag{2.2}$$

The ensemble, in which the momenta are integrated, is a surface of an n-dimensional sphere of radius $\sqrt{n}$, that we obtain normalization of the n-dimensional spin vector such that

$$|\boldsymbol{s}_i|^2 = n. \tag{2.3}$$

We can also see that the trace of the spin product (the Greek letters runs over the n-dimensions, while the Latin one's labels the position on the lattice) $s^\alpha s^\beta \dots$ is related to the generating function:

$$G(\boldsymbol{k}) = \langle \exp(-i\boldsymbol{k} \cdot \boldsymbol{s}) \rangle, \tag{2.4}$$

through the derivative of this function in $k = 0$ gives the various momenta:

$$\langle s^\alpha s^\beta \rangle = \left(-i\frac{\partial}{\partial k^\alpha}\right)\left(-i\frac{\partial}{\partial k^\beta}\right) G(k)\Big|_{k=0} \tag{2.5}$$

Thanks to $O(n)$ symmetry any odd product of spin

$$\int s_\alpha^{2n+1}\, d\Omega = 0 \qquad \forall n, \tag{2.6}$$

where $\mathrm{d}\Omega$ is the element of the surface of the n-dimensional sphere of radius $\sqrt{n}$. Also, it's easy to see that

$$\mathrm{Tr}\, s_\alpha s_\beta = \delta_{\alpha\beta}, \tag{2.7}$$

which, in the limit of $n \to 0$, is the only non vanishing term.

To prove that the all other momenta vanish in the limit we construct explicitly the generating function and show that is quadratic in k.
The laplacian of the generating function

$$\nabla^2 G := \sum_\alpha \frac{\partial^2 G}{\partial k_\alpha^2} = -\langle s_\alpha^2 \exp(i\boldsymbol{k}\cdot\boldsymbol{s})\rangle = -nG \tag{2.8}$$

where in the last passage we have used the normalization (1.7).

Since we are integrating over the spin vector, the generating function depends only on $k = |\boldsymbol{k}|$. We can express the laplacian as derivative of k:

$$\nabla^2 G = \left(\frac{n-1}{k}\right)\frac{\partial G}{\partial k} + \frac{\partial^2 G}{\partial k^2}. \tag{2.9}$$

Now inserting this in (2.8) we obtain:

$$\frac{\partial^2 G}{\partial k^2} + \left(\frac{n-1}{k}\right)\frac{\partial G}{\partial k} + nG = 0 \tag{2.10}$$

To solve this differential equation we impose the following boundary condition:

$$G(k=0) = 1 \tag{2.11}$$

$$\frac{\partial G}{\partial k}(k=0) = 0 \tag{2.12}$$

The second condition say that $G(k)$ is regular and even at small k.
We can now construct the analytical continuation for all values of n and solve it in the case $n = 0$:

$$\frac{d^2G}{dk^2} - \frac{1}{k}\frac{dG}{dk} = 0 \tag{2.13}$$

The solution to ((2.13)) is:

$$G(k) = 1 + \frac{k^2}{2} \tag{2.14}$$

since there are no power higher than k^2, it means that all the moments higher than second one must vanish.

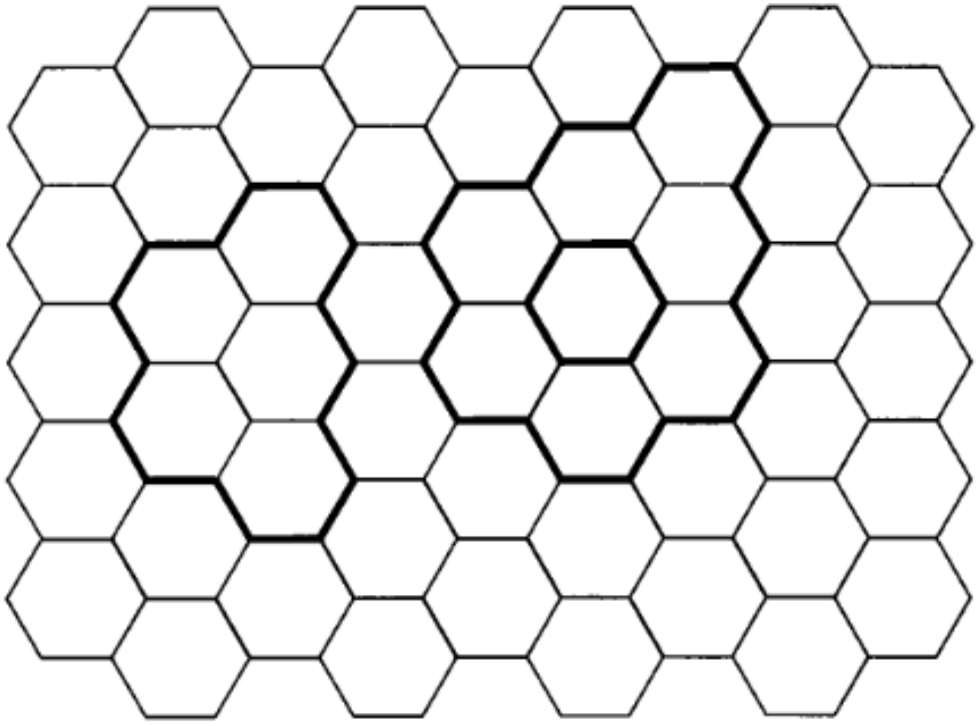

Figure 2.2: Graphs in the expansion of the partition function on the hexagonal lattice

Now we can expand in series for small coupling constant the partition function and obtain:

$$\begin{aligned} Z &= \mathrm{Tr} \prod_{\langle ij \rangle} \exp\left(K_{ij} \sum_{\alpha} s_i^{\alpha} s_j^{\alpha} \right) \\ &= \mathrm{Tr} \prod_{\langle ij \rangle} \left(1 + K_{ij} \sum_{\alpha} s_i^{\alpha} s_j^{\alpha} \right) \end{aligned} \tag{2.15}$$

This is an expansion at high temperature and any term can be represented as a graph in this lattice. Using (2.7) and knowing higher momenta vanish, we concludes that the only contributing terms are SAPs.

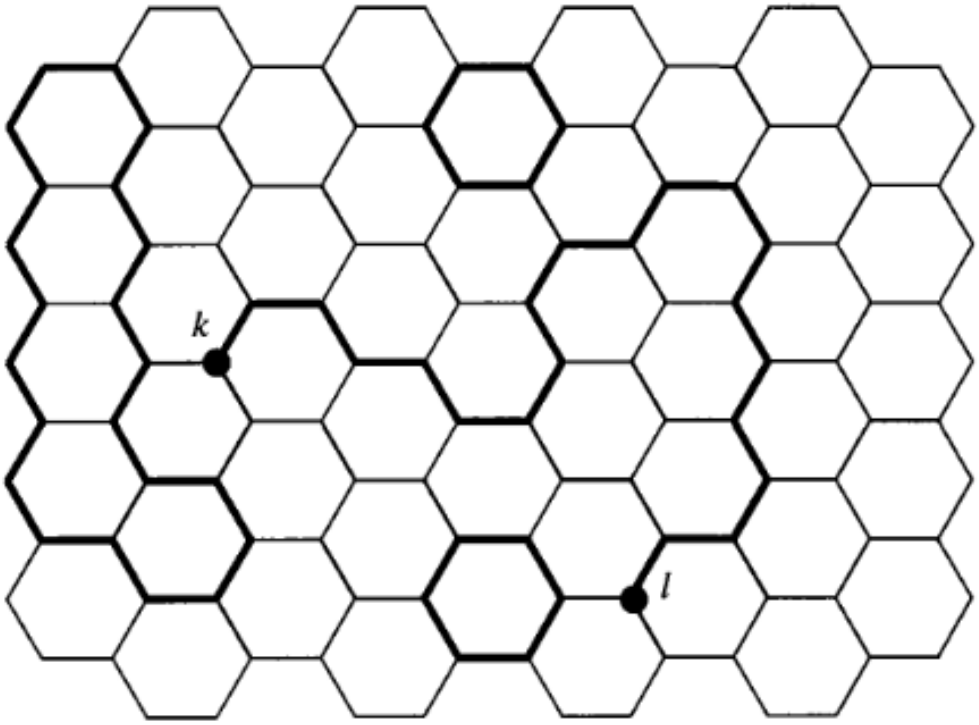

Figure 2.3: Some of the graph contributing to the spin-spin correlation function (the SAPs are eliminated dividing by Z)

2.1.1 SAWs

We have just seen how to expand the partition function in terms of SAPs; now let see how SAWs appears when calculating the spin-spin correlation function; for two spins at site i and j the correlation function it is

$$G(i,j) := \langle s_i s_j \rangle = \frac{\mathrm{Tr} s_i s_j \exp(-\beta H)}{Z}, \tag{2.16}$$

where the quantity in the angle brackets is the thermal average:

$$\langle s_i^\alpha s_l^\alpha \dots s_j^\omega s_k^\omega \rangle = \frac{\mathrm{Tr}\ s_i^\alpha s_l^\alpha \dots s_j^\omega s_k^\omega \exp(-\beta H)}{Z}. \tag{2.17}$$

Differently from the previous case in the expansion at high temperature we can't have any closed loop, because of the two extra spins; the only graphs contributing are all the SAWs that connect site i to site j.
It can be shown that each SAW (in the case the coupling constant equal for every site) contributes with a factor K^N where N is the number of edges of the graph embedded. We can now write the following important result:

$$G(i,j) = \sum_N c_{ij}(N) K^N \tag{2.18}$$

where $C_{ij}(N)$ is the number of the N-step SAW connecting site i to site j.

Any topology can be generated using a correlation function in the $n \to 0$ model, for example consider $\langle s_1^\alpha s_2^\alpha s_3^\beta s_4^\beta s_5^\gamma s_6^\gamma \rangle$ defined in a lattice such that 1,3,5 are neighbour of the origin labeled 0. In this case the graphs contributing are all 3 star with terminal vertices in 2,4,6.; it has been proven that in the limit for large distances between the points the three vertices of the single chains can be seen as one renormalized vertex with three legs.
Other important diagram is the watermelon one that has two vertices each of one have degree L: in figure the spin correlation function that describe the polymer topology is $\langle s_k^\alpha s_l^\alpha s_i^\beta s_j^\beta s_i^\gamma s_j^\gamma \rangle$.

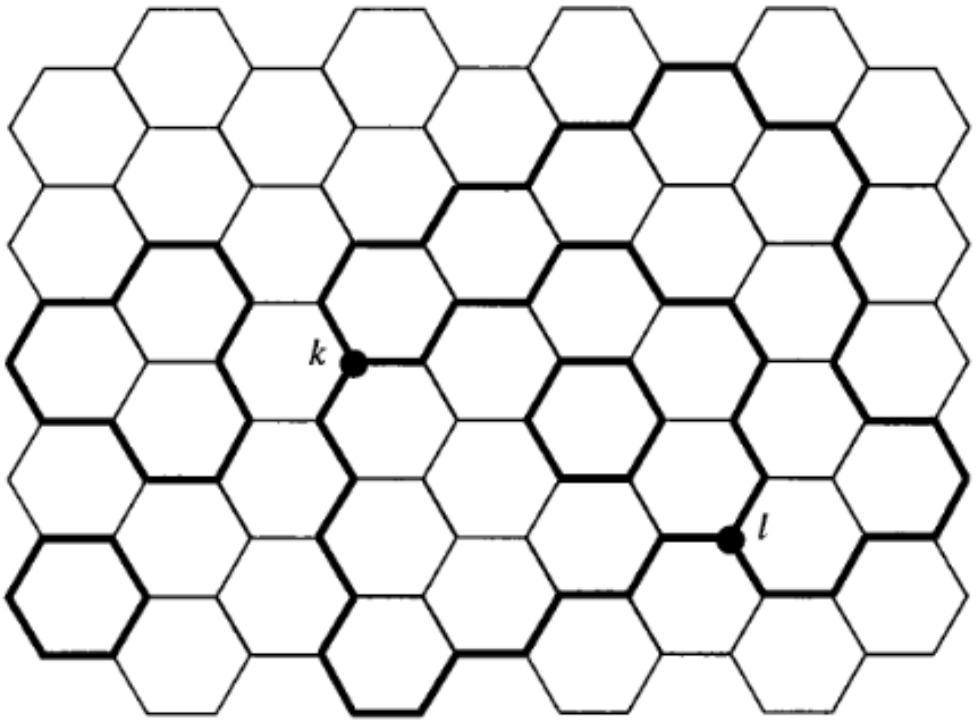

Figure 2.4: Some of the graphs contributing to the watermelon correlation function

2.2 Critical exponent

In the precedent section we have seen that polymers can be described by a ferromagnetic models with $n = 0$; this tell us that there is a critical point where thermodynamics properties behave in a non analytical way.
The equivalence of the two models tells us that the SAWs exponent are like the ferromagnetic exponents, and that allows us to use the methods to study critical behaviour to the polymer.
All the critical exponent are universal and depends only on the dimension of the lattice.

In order to obtain the grand partition function for SAWs, that is equal to the suscebility function, we have to sum over all path originating from the origin, because the function is invariant for translation.

$$\chi(K) := \sum_j G(0,j) = \sum_{j,N} c_{0j}(N) K^N = \sum_N c(N) K^N \tag{2.19}$$

where $c(N)$ is the total number of N-step SAWs originating from a point. The manner of divergence of the suscebility at the critical point is related to the asymptotic form of the number of SAWs for large N.
While the subdominant behaviour of c_N has not been established rigorously, it's assumed that the asymptotic is:

$$c_N \approx \mu^N N^{\gamma-1} \tag{2.20}$$

and therefore we expect that the $\chi_K(i)$ have the following form:

$$\chi(K) = \sum_N c(N) K^N \sim (K - K_c)^{-\gamma} \tag{2.21}$$

where $K_c = \mu^{-1}$ and this is referred as the critical point, since it's role is similar to the critical point in statistical mechanical systems.

Other quantity that diverge as approaching the critical point is the correlation length ξ, that in the polymer diverge as the average distance between vertices:

$$\xi(K) \approx (K - K_c)^{-\nu} \tag{2.22}$$

We have the same exponent for the gyration radius, which has an asymptotic behaviour:

$$R_g^2 \sim N^{2\nu} \tag{2.23}$$

It exits an effective, but non rigorous, method, called the Flory argument, for computing the exponent ν. It gives good results and it's very used for practical purposes; the argument gives us as result the following relation:

$$\nu = \frac{3}{2+d} \tag{2.24}$$

where d is number of the dimensions.

Chapter 3

Knots

In this section 1 we have discussed the case in which the polymer is under some geometrical constraints. The critical behaviour in these cases is well known and has been explored [6].

The configurational entropy of the polymer depends on the topology of the network, e.g. the presence of vertices of degree ≥ 3 or the existence of a knot. It's widely known that knots can occur on circular DNA and the presence of the knot can affect the dynamic, e.g. it can be an obstacle to the translocation of the polymer through a narrow passage: it slows the ejection times of viral DNA into the host cell.

3.1 Basic properties

Mathematically a knot is an embedding of a closed curve in $\mathbb{R}^3$ up to ambient isotopy; it means that two knots K_1 and K_2 are equivalent when there is an ambient isotopy which move K_1 to K_2. An ambient isotopy is a continous deformation of a curve trough the space (ambient) in which is embedded.In other words, instead of deforming knots alone, we deform the whole space in which they are.
While with an isotopy each knot would be found equivalent to the circle S^1, with an ambient isotopy we have a continuous deformation in the space in which the curve is embedded. This definition corresponds to our intuitive notion of knot in which we take a string, tie a knot and stick together the ends, then it's impossible to undo the knot unless we cut the string.

In order to exclude pathological cases, such as wild knots, we will consider

only knots in the same equivalence class of a polygonal curve in $\mathbb{R}^3$ (tame or simply knots).

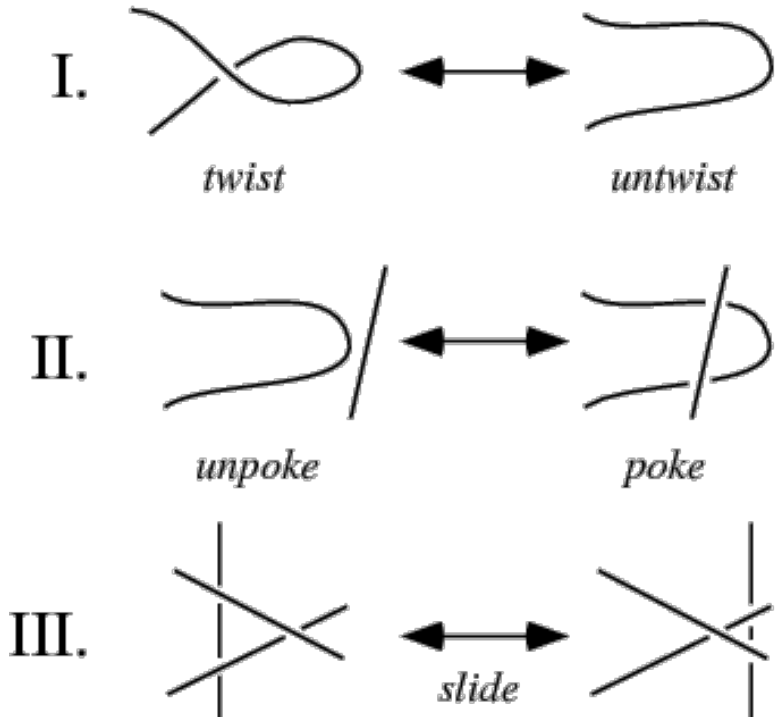

Figure 3.1: These are the three possible Reidemenster moves

3.1.1 Equivalence between knots

Given a closed curve, to identify its knot type one usually considers its projections onto a plane,a knot diagram. These planar projections are injective, expect for a finite number of crossing points; in these transverse point the branch passing "under" the other is interrupted.

All knots deformations in $\mathbb{R}^3$ can be reduced to three possible Reidemenster moves on the projection plane:

- twist $\leftrightarrow$ untwist
- unpoke $\leftrightarrow$ poke
- slide

It was proven by the Reidemenster's theorem that the previous moves correspond to ambient isotopy,in fact it states that two knots are equivalent if and only if any diagram of one knot can be transformed into a diagram of the other one by a sequence of these moves.

A given knot type have different planar projection and number of crossing, but it's possible to minimize the number of crossing compatible to that knot type. This gives us a minimal knot diagram having the smallest number of crossing $n_{cr}^{\min}$.
This value is used to classify the knots in groups of increasing topological complexity: the unknotted configuration is associated to $n_{cr}^{\min} = 0$, the next one is the trefoil knot $n_{cr}^{\min} = 3$, then we have figure-eight knot $n_{cr}^{\min} = 4$, etc (see Fig 3.2).
As the minimal number of crossing increases, also the topologically different knots increase this are usually distinguished by a subscript, for example for the two 5-crossing knots, 5_1 and 5_2.

Note that even if the number of crossing n_c^{min} is a useful tool to classify knots isn't enough to distinguish between knot types (e.g. 5_1 and 5_2 have the same n_c^{min} but they're different knots).

3.1.2 Prime and composite knots

As one can experience with a string a non-trivial knot K can't be untied by tying another non-trivial knot K' in the string; it's impossible to manipulate the double knot in order to obtain the unknotted rope. In this sense intuitively we can say that there aren't any anti-knots, indeed it has been proven that the composition of any number of knots cannot result in the unknot unless each knot is the unknot [13].
Denoting by $K\#K'$ the composition of K and K', it has been proven [13] that

$$n_{cr}^{\min}(K\#K') \leq n_{cr}^{\min}(K) + n_{cr}^{\min}(K) \tag{3.1}$$

It's still conjuctered if the equality holds.
The connected sum with the oriented knots forms a monoid with the unknot as the identity element, furthermore it has the following properties:

- the operation is commutative
- each not trivial knot has a unique factorization in prime knots

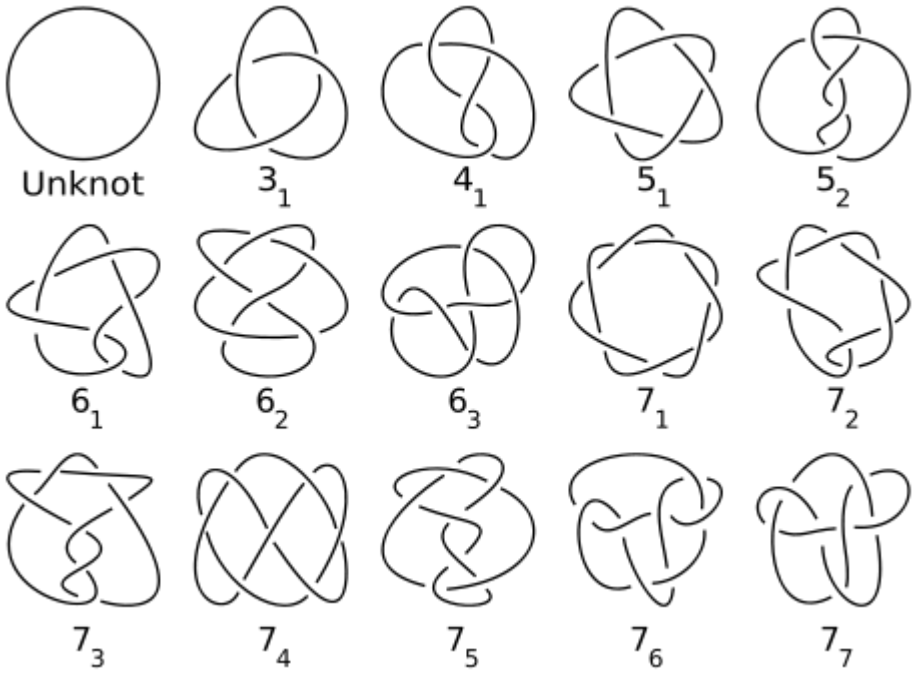

Figure 3.2: Prime knots with minimal number of crossing up to 7 (enantiomer aren't considered in this table)

(a) 3#4 (b) 3#0

Figure 3.3: In the figure (a) is shown the connected sum of two knots and in the (b) is shown that the identity element is the unknot

3.1.3 Chirality

In the previous discussions we have neglected enantiomorphs even if has been proved that there are knots that are not equivalent to their mirror image. The knots that can't be continuously deformed into another are said to be chiral, while the one that are equivalent to their mirror image are said achiral. Most of knots are chiral, the simplest chiral knot is the trefoil one, instead the achiral ones are quite rare, these includes the ring and the 4-crossing knot.

Figure 3.4: The first chiral knot is the trefoil, while the first achiral (except for the unknot) is the 4-crossing knot

3.2 Partition function

In the previous chapters we have discussed the asymptotic form of the partition function for SAWs. Now we want to focus on the problem of ring polymers (that are classes of SAPs), that are particular interesting in the field of biophysics.
Since physically the self-crossing is forbidden, we want the partition function for SAPs with a particular knot type.

3.2.1 Unknot configurations

It strongly assumed that for large N for SAPs with a particular knot type k that:

$$Z_k(N) = A_k \mu_k^N N^{\alpha_k - 2} \tag{3.2}$$

There isn't any relation between μ_k and μ, but is it possible to prove that for the unknotted SAPs, $k = 0$, that $\mu_0 < \mu$, while for the entropic exponent α_0 the numerical results suggest that $\alpha_0 = \alpha$, but the results are not enough

to exclude a small difference.

As we have said before the probability of finding a knot grows with the number of monomer. The probability of a unknot configuration in the ensemble is given by

$$P_0(N) = \frac{Z_0(N)}{Z(N)} \tag{3.3}$$

where the $Z(N)$ counts all possible configuration in the ensemble of the SAPs, while $Z_0(N)$ counts the configuration in the subensemble of the unknots. Using the relation (3.2), we obtain that for large N the probability seems to have the following behaviour:

$$P_0(N) \simeq \frac{A_k}{A}\left(\frac{\mu_0}{\mu}\right)^N N^{\alpha_0-2} = \frac{A_k}{A} e^{-N/N_0} N^{\alpha_0-2} \tag{3.4}$$

where $N_0 = \frac{1}{\ln \mu/\mu_0}$ gives the typical scale above which the presence of knots is no more negligible. Since $\mu_0 < \mu$ we notice that the probability of finding an unknot configuration goes to zero exponentially with N.

3.2.2 Knotted configuration

For the frequency of the knotted configuration there is no analytical result, we have to rely on numerical results. Using techniques on lattice that preserves the topology of the polymers they have found that is strongly assumed that the connective constant for a knotted configuration is the same of the unknotted one:

$$\mu_0 = \mu_k < \mu \tag{3.5}$$

There are evidence that the presence of knots vary the critical exponent α, in fact we have supposed the following relation:

$$\alpha_k = \alpha_0 + n_k \tag{3.6}$$

where n_k is the number of prime knots in the polymer. This relation is consistent to the fact that for large N prime knots are weakly localized, that means the knot can be found in any point of the polymer. So in swollen rings the prime knots can be considered as a special vertex that can move along

the unknotted ring, this can be seen as an additional degree of freedom and it brings a factor N for each prime knot in front of Z_0, so for large N the partition function can be written as:

$$Z_k(N) \simeq N^{n_k} Z_0(N) \tag{3.7}$$

This relation is quite raw, in fact it doesn't consider the amplitude A_k that does depends on the kind of knot considered and not only the number of prime knots in the factorization.

Chapter 4

Computational model

In this chapter we describe the coarse-grained polymer chain model we use and the molecular dynamics (MD) techniques we use to simulate a polymer in a in equilibrium with a thermic bath at temperature T.

MD is a numerical technique used to integrate Newton equation of motion for molecular system, from fluids to biomolecules.

4.1 Bead spring model

To model a polymer we consider a chain of impenetrable beads kept together by a quasiharmonic potential.
To illustrate how the course-graining procedure work, we report in Fig. 4.1 a

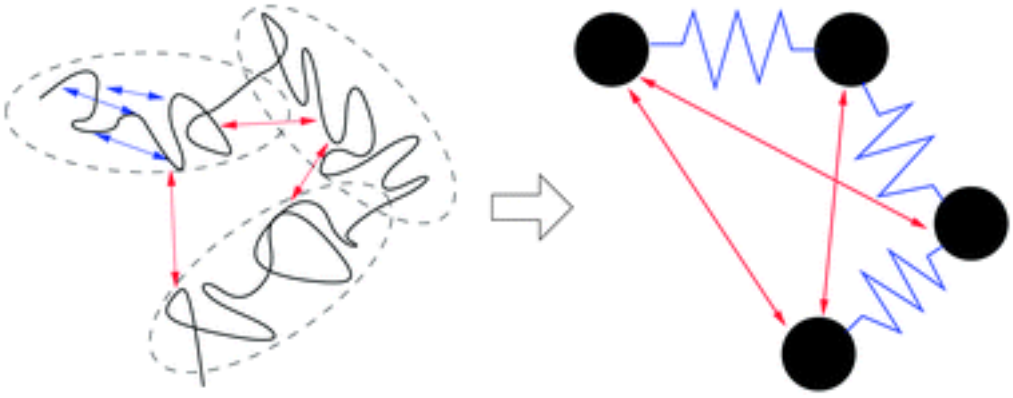

Figure 4.1: In the figure we see the course-graining for a polymer chain, now the chain is represented by the bead spring model

cartoon. The process of couse-graining reduces the complexity of the system:

for a molecule of polyethylene with 300 monomers (CH_2) can be replaced by a chain with 100 identical course-grained beads.
This simplification gives various advantages: it makes possible to simulate bigger systems, with more chains or loner one, and it allows to perform simulation for longer times. This permits to use larger time step due to the fact that course-grained potential are softer than the atomic ones and it prevents to the MD simulation to explode or become unstable.

4.2 Equations of motion

The classical MD techniques consists in a stepwise integration of Newton's equations for an N particle system:

$$m\frac{d^2\boldsymbol{r_i}}{dt^2} = \boldsymbol{F}_i(\boldsymbol{r}_1, \ldots, \boldsymbol{r}_N) \tag{4.1}$$

where $\boldsymbol{r}_i$ is the position of the i-th particle on which it's exerted a force $\boldsymbol{F}_i$

$$\boldsymbol{F}_i(\boldsymbol{r}_1, \ldots, \boldsymbol{r}_N) = -\nabla_i \left(\sum_{i \neq j} U_{ij} \right) \tag{4.2}$$

The total energy of the system is conserved and the trajectory obtained solving the (4.1) is consistent with the microcanonical ensemble; the simulation performs a NVE-constant integration (number, volume, energy). To simulate a system in the canonical ensemble we consider the system in contact with a bath, this corresponds to add in (4.1) the interaction with the solvent particles. The equations of motion are the so called Langevin equations:

$$m\frac{d^2\boldsymbol{r}_i}{dt^2} = -\frac{1}{\eta} v_i - \nabla_i \left(\sum_{i \neq j} U_{ij} \right) + \mathcal{F}_i(t) \tag{4.3}$$

where η is the damp constant and $\mathcal{F}(t)$ is a Gaussian noise term with zero-mean (the averages are taken respect to the ensemble considered):

$$\langle \mathcal{F}_i(t) \rangle = 0 \tag{4.4}$$

and the following correlation function

$$\langle \mathcal{F}_i(t) \mathcal{F}_j(t') \rangle = \frac{2k_b T}{\eta} \delta_{ij} \delta(t - t') \tag{4.5}$$

4.3 Potential

A proper choice of the force fields describe the effective interaction between particles.
The most important pair interaction is the Lennard-Jones potential:

$$V_{LJ}(r) = 4\epsilon \left[\left(\frac{\sigma}{r}\right)^{12} - \left(\frac{\sigma}{r}\right)^{6} \right] \tag{4.6}$$

where $\boldsymbol{r}$ is the distance between non consecutive (along the chain) beads, ϵ is the minimum energy and σ is the distance at which $V_{LJ}(\sigma) = 0$, as depicted in Fig. 4.2. This potential have a repulsive hard core interaction that dominates at short range ($\propto r^{-12}$) and a weakly attractive tail ($\propto r^{-6}$).
It's often useful to consider only the repulsive part of the LJ potential. In order to obtain this kind of interaction the LJ is truncated at a cut-off distance that corresponds to the position of the minimum and it's shifted such that $V_{new}(2^{1/6}\sigma) = 0$. This result is known as the Weeks-Chandlers-Andersen, WCA, potential:

$$V_{WCA} = \begin{cases} 4\epsilon \left[\left(\frac{\sigma}{r}\right)^{12} - \left(\frac{\sigma}{r}\right)^{6} \right] + \epsilon & \text{for} \quad r < 2^{1/6}\sigma \\ 0 & \text{otherwise} \end{cases} \tag{4.7}$$

and is reported as a dashed curve in Fig. 4.2

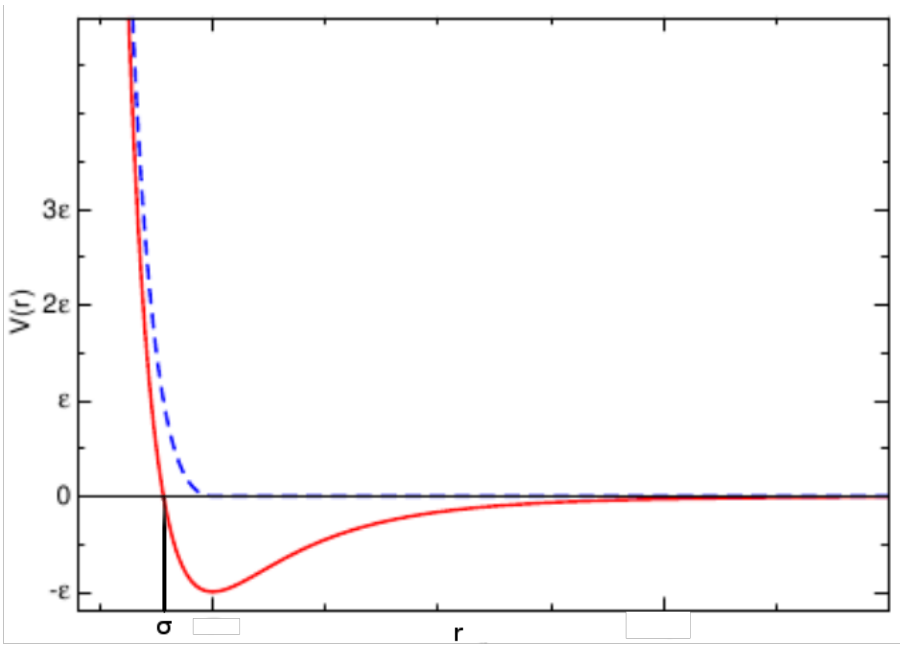

Figure 4.2: In red there is represented the Lennard-Jones potential and in blue the WCA potential

For polymeric system the WCA potential is a good choice to reproduce the excluded volume interaction. In fact in this way the beads are effective hard-core sphere of diameter about $r \approx \sigma$.

To describe the connectivity of the polymer along the chain we use the combination of two potential (see Fig 4.4): WCA potential accounts for the excluded volume effect between consecutive beads and a attractive interaction which is given by a FENE (Finite Extensible Nonlinear Elastic) interaction

$$U_{FENE}(r) = -\frac{1}{2}k_b \Delta R^2 \ln\left(1 - \frac{(r - R_0)^2}{\Delta R^2}\right) \tag{4.8}$$

where k_b is the spring constant, R_0 is the rest length and ΔR is the maximum extent of the bond (see Fig. 4.3).

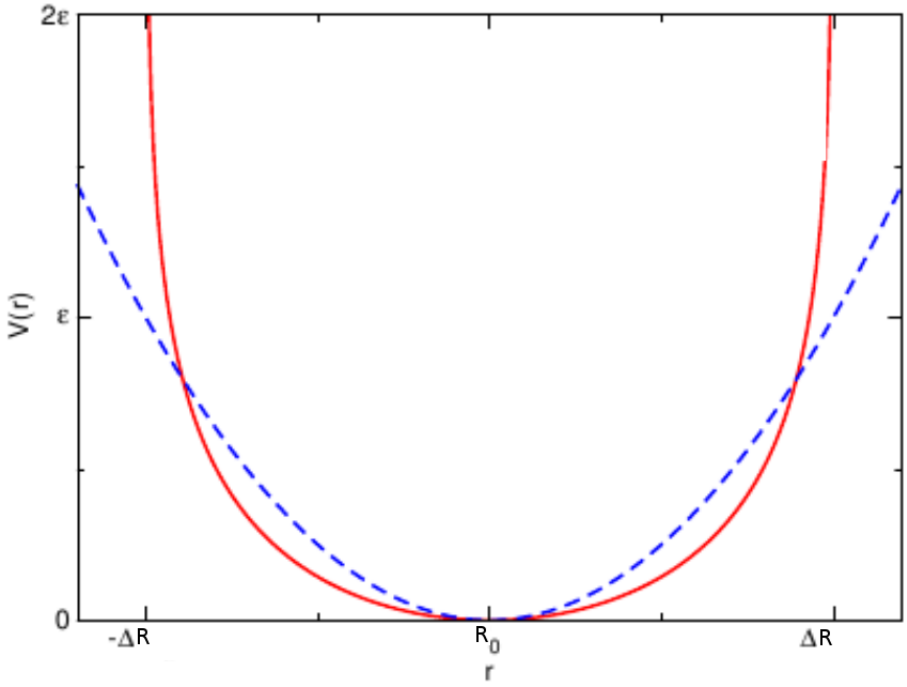

Figure 4.3: The full line is the FENE potential and the dashed line is the harmonic potential

This potential models a non linear spring and near the rest length R_0.

$$U(r) \approx \frac{1}{2}k_b(r - R_0)^2 \tag{4.9}$$

Chain self-crossing is energetically unfavorable and the simulation preserves the topology of the chain.

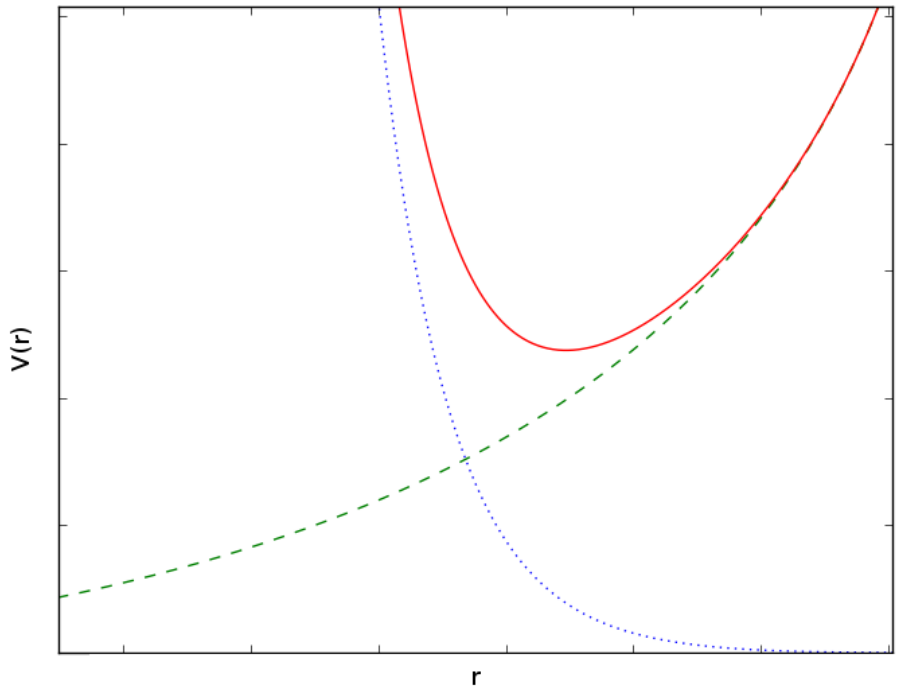

Figure 4.4: The dotted line is the WCA potential, the dashed one is the FENE potential and the solid one is the sum of the two

We must consider the interactions between the polymer and the wall. The latter is composed by unmovable atoms placed in an hexagonal lattice (see Fig. 4.5) which, since the wall is completely repulsive, interact with the beads along the chain with a WCA potential.
In order to make the translocation possible we have realized an hole in the membrane by removing an atom from the lattice

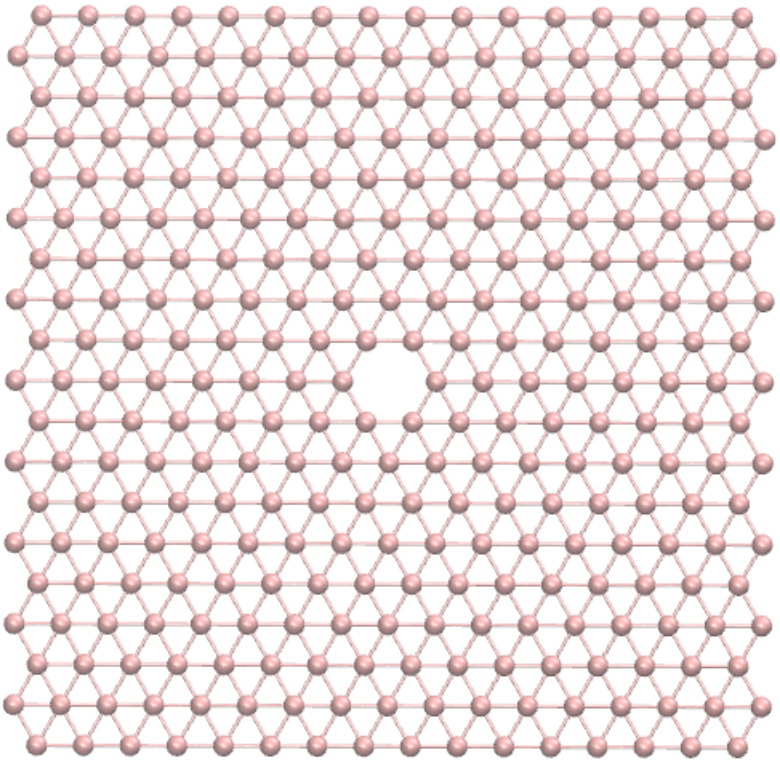

Figure 4.5: The beads mimic a completely impenetrable membrane

4.4 LJ units

During MD simulations it's difficult to express physical quantity using the units of the international system (SI). We're looking to a new units that allow to extent the results to different systems and in order to make easier calculation and avoid operation that could lead to underflow or overflow.
When we use Lennard-Jones potential choosing σ and ϵ as basic unit of length and energy ($\sigma = 1$, $\epsilon = 1$) seems appropriate. With the bead mass $m = 1.0$ these are the basic MD units and other physical quantities are expressed in derived unit.

Quantity	LJ unit	SI unit for CH_2	SI unit for Ne
length	σ	$0.39\,\mathrm{nm}$	$0.27\,\mathrm{nm}$
energy	ϵ	$0.83 \times 10^{-21}\,\mathrm{J}$	$0.50 \times 10^{-21}\,\mathrm{J}$
mass	m	$14\,\mathrm{g/mol}$	$20.2\,\mathrm{g/mol}$
time	$\sigma(m/\epsilon)^{1/2}$	$2.01\,\mathrm{ps}$	$2.21\,\mathrm{ps}$
temperature	ϵ/k_b	$60.4\,\mathrm{K}$	$36.2\,\mathrm{K}$
velocity	$(\epsilon/m)^{1/2}$	$1.89 \times 10^2\,\mathrm{m/s}$	$1.22 \times 10^2\,\mathrm{m/s}$

Table 4.1: Some physical quantities expressed in Lennard-Jones unit and SI units

In table 4.1 there are some examples of physical quantities in LJ units and SI units: we have investigated the case for a unit of polyethylene (CH_2 and for an atom of Ne gas. In LJ units the Boltzmann constant is equal to $k_b = 1.0$.

It's quite a delicate task the relation between experimental and computational results. The relation between SI units and LJ units is not exact and it's possible to have only the characteristic magnitudes of these relations, so became difficult to correlate numerical predictions to the experimental results obtained in laboratory. Even if there is not an exact correspondence, the computational results obtained can give extremely valuable insight regarding scaling laws and the statistical behaviour of the interacting systems.

4.5 Integration scheme

The integration of the Newton's equation of motion is performed trough the velocity Verlet integration scheme:

1. Calculate
$$\boldsymbol{v}\left(t + \frac{1}{2}\Delta t\right) = \boldsymbol{v}(t) + \frac{1}{2}\boldsymbol{a}(t)\Delta t \tag{4.10}$$

2. Calculate
$$\boldsymbol{r}(t + \Delta t) = \boldsymbol{r}(t) + \boldsymbol{v}\left(t + \frac{1}{2}\Delta t\right)\Delta t \tag{4.11}$$

3. Derive $\boldsymbol{a}(t + \Delta t)$ using the updated velocities and position

4. Calculate
$$\boldsymbol{v}(t + \Delta t) = \boldsymbol{v}(t) + \frac{1}{2}(\boldsymbol{a}(t) + \boldsymbol{a}(t + \Delta t))\Delta t \tag{4.12}$$

This kind of integration satisfies the time-reversibility (i.e. the conservation of the energy). In the previous algorithm we have assumed that the acceleration only depends on the position and not to the velocity.

4.6 Thermostats

Since we are working in the canonical ensemble (NVT) we have to introduce a thermostat to modulate and keep constant the temperature of the system. There are various ways to implement it, in our simulation we use the Langevin thermostat.
The Langevin equation can be used for molecular dynamics by assuming that the atoms being simulated are embedded in a virtual heath bath. In many instances the interaction between solvent-solute is not interesting and the solvent particles interact with the solute via random collisions and imposing a frictional drag force.

Obviously the immediate advantage for this thermostat is that we eliminate many atoms and include them in the stochastic term.
Beside, the Langevin thermostat is very suitable for simulating polymeric system for which long time simulation is needed. Due to the dissipative term the MD simulation accept larger time step, because the damping term stabilizes the equation of motion. Furthermore, the stochastic term replaces the fastest frequency motions, this allows us to resolve slower degree of freedom.

4.7 Initialization and equilibration

The polymer chain is placed in a simulation box of dimension $L_y = L_z = 34$ and $L_x = 68$ (the x axis is orthogonal to the wall) with periodic boundary conditions. In order to be able to perform an interesting MD simulation, the polymer system have to be initialized. The The beads in the hole are kept fixed (see the bigger bead in Fig 4.6), such that the number of monomers in each half space are kept constant.

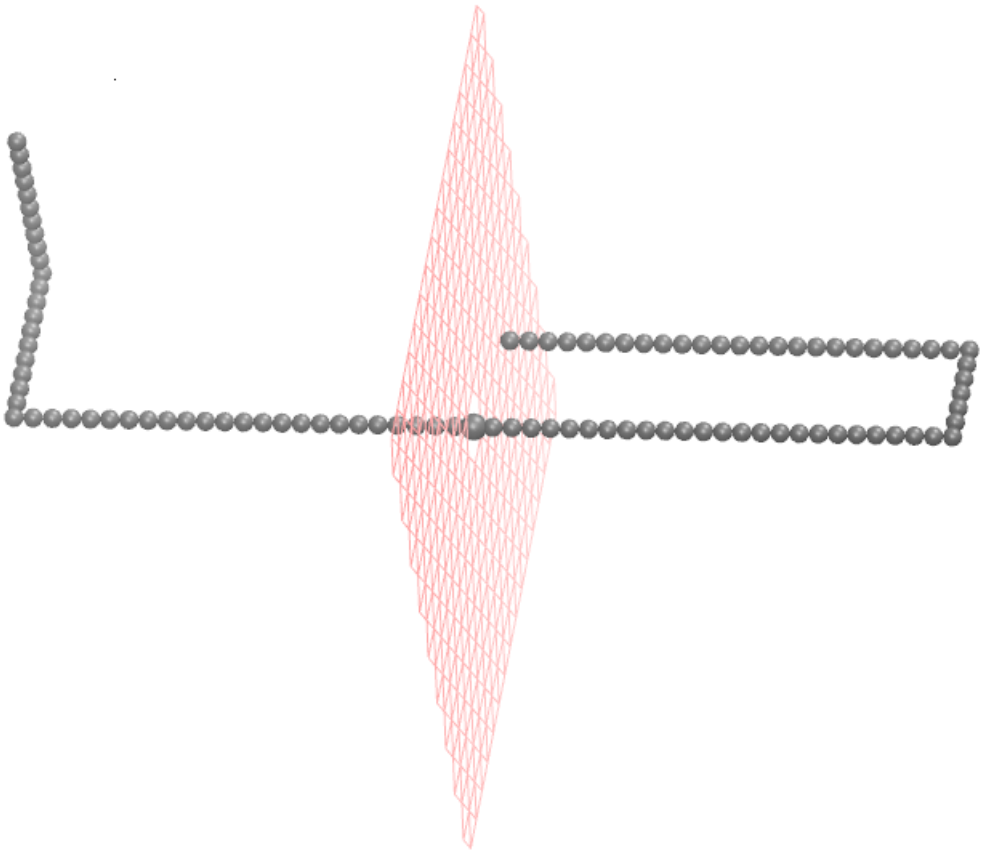

Figure 4.6: A typical initial condition

Then we perform a pre-equilibrating MD run in which we employ the potentials discussed above, but it is imposed a maximum distance an atom can move in one timestep. This is useful to eliminate the initial beads overlap that can induce numerical instabilities, if the atoms are overlapped this would generate a huge force which would blow them out the simulation box. Even if in our case there are not overlapped beads in our initial data, it is recommended to perform this procedure to reach an equilibrium configuration, see Fig 4.7.

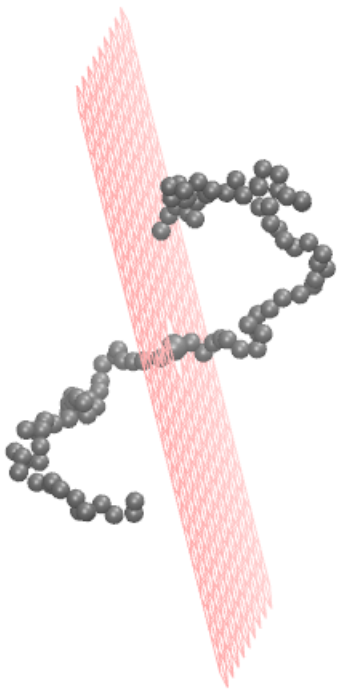

Figure 4.7: An equilbrium configuration reached after the pre-equilibrating MD run

For the simulation of polymeric systems we use a software called LAMMPS: Large-scale Atomic/Molecular Massively Parallel Simulator developed at Sandia National Laboratory. We develop a script that is read by LAMMPS, in which we specify the features of our polymer system (i.e. the initial position and velocities, the forces, the method of integration ...).

4.8 Simulation's details

The parameters given in this section are written in LJ units.
Each bead in the simulation have unitary mass:

$$m = 1.0 \tag{4.13}$$

The bond is a FENE between polymer has these parameter:

$$R_0 = 1.7 \quad k = 200.0 \quad \epsilon = 1.0 \quad \sigma = 1.0 \tag{4.14}$$

The self avoiding effect is reproduced by a WCA with the following parameters:

$$\epsilon = 1.0 \quad \sigma = 1.0 \tag{4.15}$$

The repulsive wall's beads interacts with the monomers of the polymer with a WCA:

$$\epsilon = 1.0 \quad \sigma = 2.0 \tag{4.16}$$

The distance beetwen the beads in the wall is $D = 2$.
All the simulation are performed with a Langevin thermostat:

$$\eta = 2.0 \quad T = 15.0 \tag{4.17}$$

The temperature is high enough in order to guarantee a good solvent behaviour (this temperature is well above the θ temperature in bulk).

The simulations are performed with a time step:

$$\Delta t = 2,5 \cdot 10^{-4} \tag{4.18}$$

Every run lasts for about $\approx 20000000/30000000$ and is performed ≈ 60 times.

Chapter 5

Results

Here we present the results concerning the translocation of a polymer with a given topology through a pore of an impermeable membrane.
In the simulation we have a membrane with a pore of diameter D, that is of the same order of the typical length of the bond, in which the polymer chain can pass through. For simplicity we have made the pore hexagonal, but we assume that the geometry of the pore doesn't affect the general behaviour. The wall is a rigid surface and is repulsive to avoid the undesired phenomena of polymer adsorption.
Note that there are no external forces acting on the polymer and the translocation we consider is based purely on polymer diffusion (unbiased translocation).
In this case it is expected that the unbalance in free energy of the polymer between the cis and the trans region would drive the translocation [16]. The free energy landscape is parametrized by the number of monomers $N - s$ already translocated.

5.1 General consideration

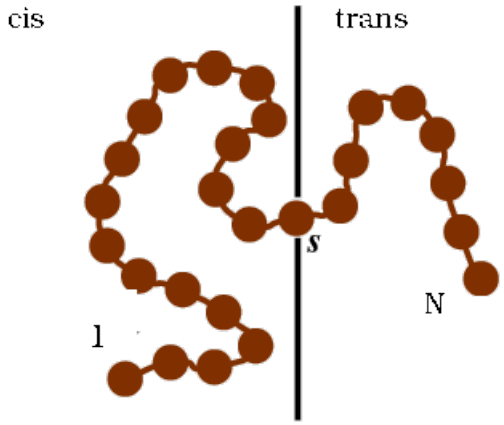

Figure 5.1: Translocation of a polymer trough a rigid membrane

In Fig. 5.1 we show a sketch of the system, with s and $N - s$ monomers respectively in the cis and one regions. Since the wall is impenetrable one considers the two sub chains as independent and the free energy of the whole system is the sum of the tethered chains

$$F(N, s) = F_{cis}(s) + F_{trans}(N - s) \tag{5.1}$$

The problem is then reduced to computation of the free energy of the chain in cis and trans parts.
In the following Note that the behaviour of the chain within the pore is not considered, the chain fragment in the pore is assumed to contribute a constant part into the total free energy. The hole is quite narrow and permits the translocation of only one bead or, at most, two (only in the case of a ring polymer).

In the following sections we will consider different topologies: linear polymer with one end anchored in the wall in the cis region (section 5.2), linear polymer with a knot 4_1 in the cis region and both end anchored in the wall, one in the cis region and one in the trans one, (section 5.3), linear polymer with a knot 4_1 in the cis region and one end anchored in the wall in the same region and in the trans region one end free to move (section 5.4), ring polymer with a knot 4_1 in the cis region and a knot 3_1 (section 5.5).

5.2 Linear polymer in bridge configuration

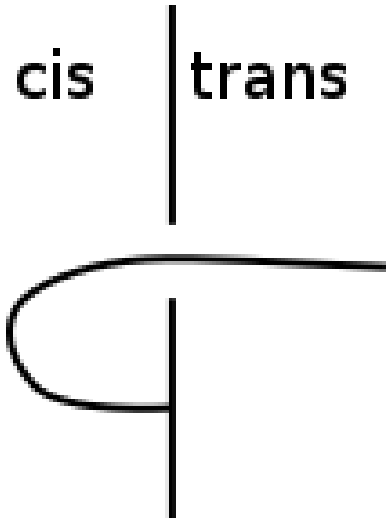

Figure 5.2: In figure there is a sketch showing the main topological features of the polymer. In the cis region the sub chain has one end attached to the wall and one fixed at the pore, while in the trans region the sub chain has one end free to move and the other fixed at the pore.

In Fig 5.2 we depict the simulation setup in which the polymer is linear and has one end anchored at the wall in the cis region. As we said before, the two sub chains are independent: in the cis region the sub chain has one end fixed at the pore while the other is anchored to the wall (bridge configuration). The sub chain in the trans region has instead one end free to move and the other is at the pore. In this case the total free energy is

$$F(N,s) = (1-\gamma_{11})\ln s + (1-\gamma_1)\ln(N-s) + \Delta\kappa s + F_0 \qquad (5.2)$$

where $\Delta\kappa$ is the difference of chemical potential of the two sub systems (the chemical potential for polymers on lattice is the logarithm of the connectivity constant).
For the cis region, we can safely assume that the dominant behaviour of the free energy is the same as the one of a ring configuration, in the thermodynamic limit the bridge is equivalent to the unknot (the case studied in chapter 3). In chapter 1 we have seen how to calculate the entropic exponents for different polymer network topologies. In this case γ_{11} is the correct entropic exponent for this subsystem , the two numbers subscripts mean that the polymer has two final vertices (degree 1) fixed on a surface.

The trans sub chain has one extremity free to move and the correct entropic exponent is γ_1 (a vertex of degree 1 attached on a surface).

Extensive simulations of this configuration allow us to sample the probability density function (PDF) of s/N,$P(s/N)$ (Fig. 5.3). The histograms does not present the typical bimodal shape [14], but for $N = 200$ it presents a behaviour suggesting that for larger N the second peak should appear.
In order to obtain the free energy we calculated $F(N, s)$ by taking the logarithm of the PDF, Fig 5.4. The location of the free energy does not depend on N.
Since Eq (5.2) is valid for large N, it cannot reproduce very well the behaviour either for small s or very close to the total length N of the polymer. In fact for short s the polymer in the cis part it's completely attached to the wall.

In order to obtain $\Delta\kappa$, we have used the free energy $F(N, s)$ calculated previously, then we have plotted in Fig. 5.5-5.7:

$$F(N, s) + (\gamma_1 - 1) \ln s + (\gamma_{11} - 1) \ln(N - s) \tag{5.3}$$

where for the critical exponents we have used the values found in literature [6] $\gamma_1 = 0.70 \pm 0.02$ and $\gamma_{11} = -0.4 \pm 0.3$. From the estimate of the angular coefficient of the linear fit, in Fig. 5.5-5.7, we get the difference of the chemical potential. The values we have obtained are tabulated in Table 5.1.

The PDF of the length of the cis sub chain shows a power-law decay $\sim s_1^x$, with $x \approx 1.7$ (see Fig 5.8). This suggest that the entropic exponent of the sub chain is $\gamma_{11}^{sim} \approx 0.7$, a value compatible to the one we have found in literature $\gamma_{11}^{lit} = 0.4 \pm 0.3$.

N	$\Delta\kappa$
100	0.0211 ± 0.0008
150	0.0243 ± 0.0006
200	0.0144 ± 0.0004

Table 5.1: Chemical potential

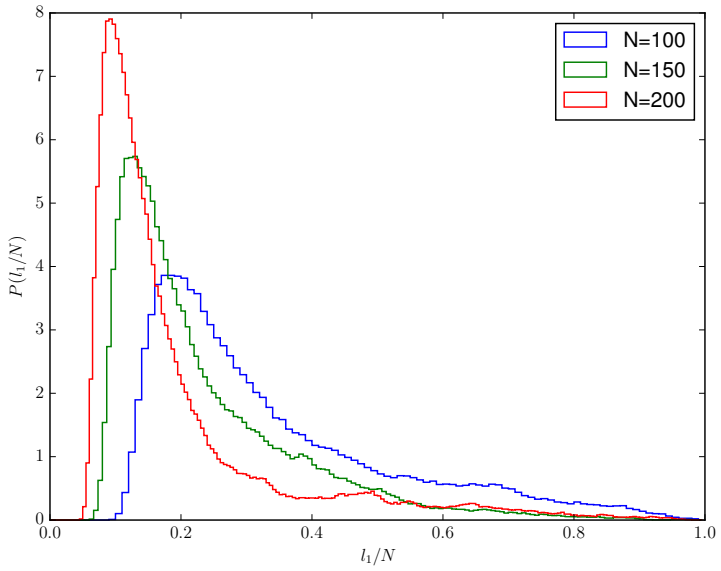

Figure 5.3: Histograms of $P(s/N)$ for cis sub-chain vs trans sub-chain (see Fig 5.2). Different curves correspond to different N values (see legend)

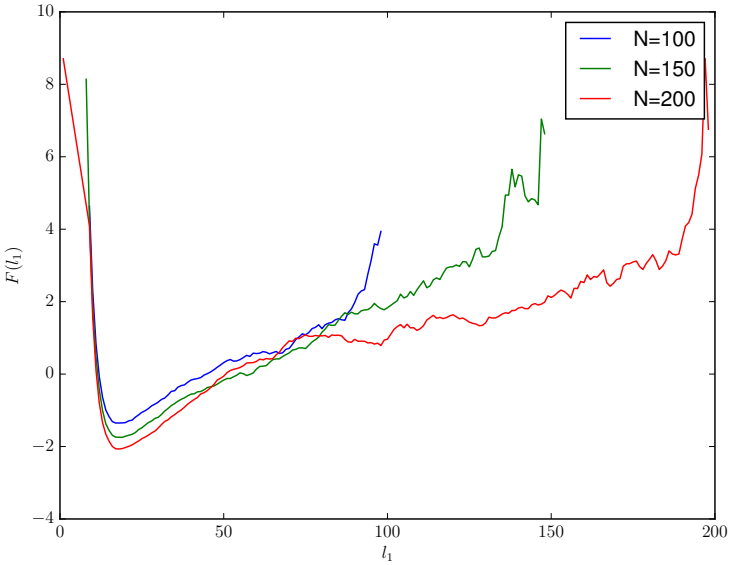

Figure 5.4: The profile of the free energy $F(s)$. Different curves correspond to different N values (see legend)

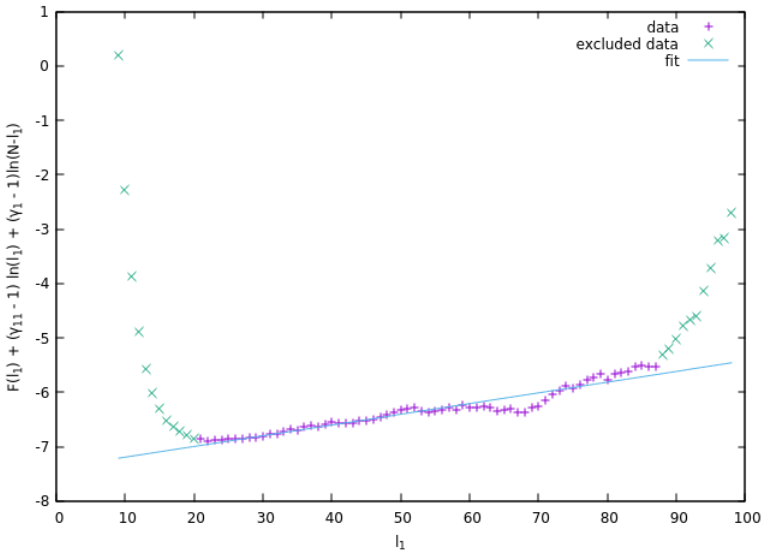

Figure 5.5: Plot of $F(N,s) + (\gamma_1 - 1)\ln s + (\gamma_{11} - 1)\ln(N-s)$ for $N = 100$. The straight line represent the linear fit, the value of its angular coefficient is the difference of chemical potential $\Delta\kappa$.

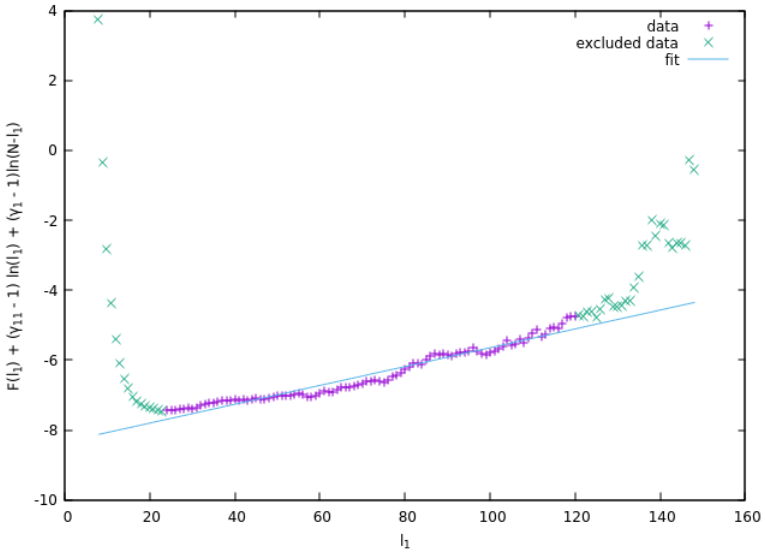

Figure 5.6: Plot of $F(N,s) + (\gamma_1 - 1)\ln s + (\gamma_{11} - 1)\ln(N-s)$ for $N = 150$. The straight line represent the linear fit, the value of its angular coefficient is the difference of chemical potential $\Delta\kappa$.

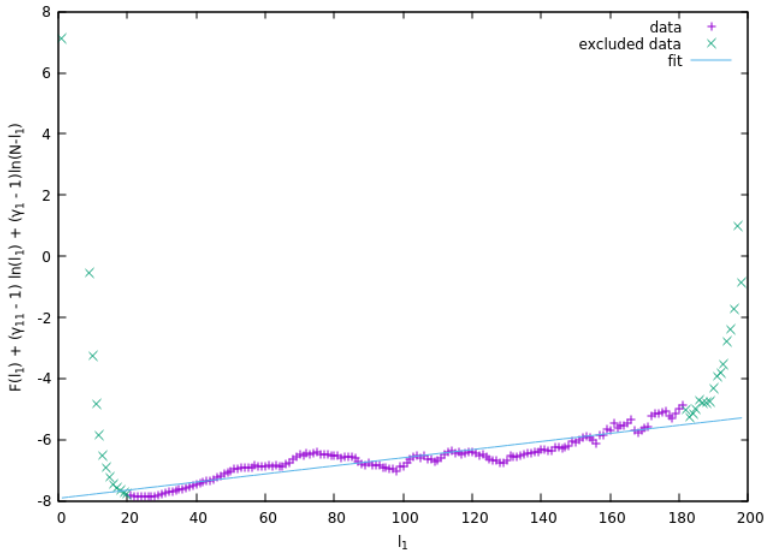

Figure 5.7: Plot of $F(N,s) + (\gamma_1 - 1)\ln s + (\gamma_{11} - 1)\ln(N-s)$ for $N = 200$. The straight line represent the linear fit, the value of its angular coefficient is the difference of chemical potential $\Delta\kappa$.

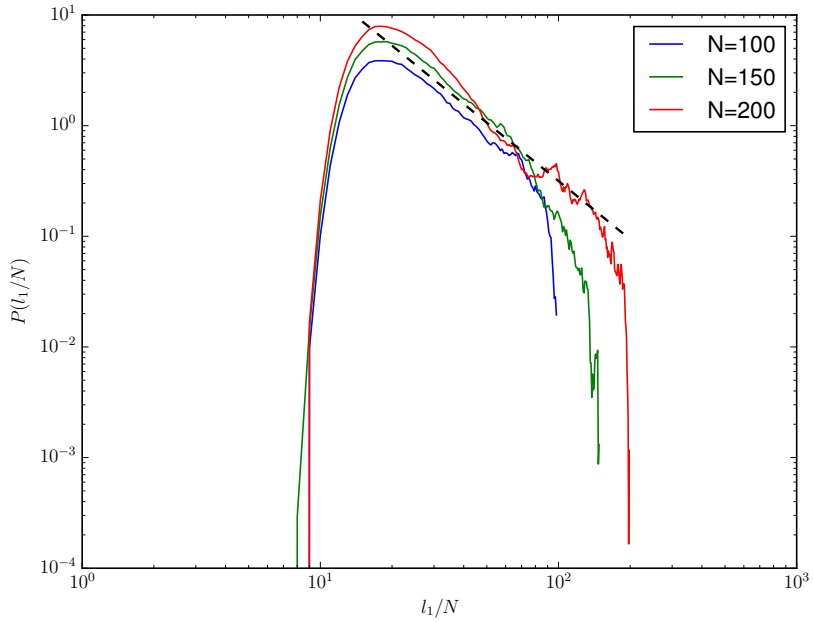

Figure 5.8: Log-log plot of $P(s)$. The dashed line represents a power law $s^{-1.7}$.

5.3 Polymer in bridge configuration with a knot 4_1

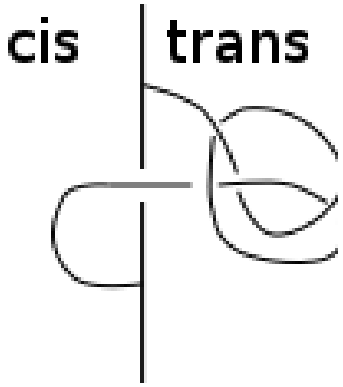

Figure 5.9: In figure there is a sketch showing the main topological features of the polymer: in the trans region the sub chain has one end attached to the wall, one fixed at the pore and has a knot 4_1, while in the cis region the sub chain has one end attached to the wall and the other fixed at the pore.

We know consider the case in which both ends of the polymer are tied and there is a knot tied in the cis region.
The topology we have in mind is the one depicted in Fig. 5.9 where in the trans compartment there is tied a figure-eight knot and both ends are fixed (one at the wall while the other at the pore), while in the cis region the sub-chain has the same configuration as the sub-chain in the cis compartment of the previous case (see section 5.2).
We have constructed the polymer in such a way that the final vertices are constrained to the wall in a symmetric point respect to the hole.

Trough simulations we have sampled the PDF of s/N (see Fig 5.10), similar to the previous case it doesn't present the bimodal shape, but there are hints that the second peak should appear as N grows.In fact, we can see from the histogram relative to $N = 200$ that the distribution becomes broader for bigger s.
From the PDF we have calculated $F(s, N)$ (see Fig. 5.11) as in the previous case and similar to that the location of the minimum of the free energy, as in the previous case, doesn't depend on N.
According to the consideration made in chapter 3 we expect that the presence

of a knot tied in the trans region modifies the entropic exponent:

$$\gamma'_{11} = \gamma_{11} + 1 \tag{5.4}$$

while the other is γ_{11} (the same of the previous section). Thus, the total free energy of this configuration is:

$$F(N, s) = (1 - \gamma_{11}) \ln s + (1 - \gamma'_{11}) \ln(N - s) + \Delta\kappa s + F_0 \tag{5.5}$$

As in the previous case we have estimated the values of $\Delta\kappa$: we have used the free energy calculated before, then we have plotted in Fig. 5.12-5.14:

$$F(N, s) + (\gamma_{11} - 1) \ln s + (\gamma'_{11} - 1) \ln(N - s) \tag{5.6}$$

The values we have obtained are tabulated in Tale 5.2. The value of $\Delta\kappa$ for $N = 200$ have been calculated for a narrow range of m: values for higher s are discarded, as for the precedent case, the statistics gathered is not sufficient to have a correct behavior of the tail.
The value of $\Delta\kappa$ decreases as N grows (see Tab 5.2), we expect, for this configuration, that for very large N it would be compatible with 0: the theory tells us that the chemical potential of the two regions is the same. Probably for small values of N the corrections to scaling, due to the finite size of the knot, are too big, so the results are strongly biased.

The PDF of the length of the cis sub chain shows a power-law decay $\sim s_1^x$, with $x \approx 1.75$ (see Fig 5.15). This suggest that the entropic exponent of the sub chain is $\gamma_{11}^{sim} \approx 0.75$, a value compatible to the one we have found in literature $\gamma_{11}^{lit} = 0.4 \pm 0.3$ and very similar to the one obtained in the previous case.

N	$\Delta\kappa$
100	0.129 ± 0.005
150	0.0276 ± 0.0009
200	0.0059 ± 0.0008

Table 5.2: Chemical potential

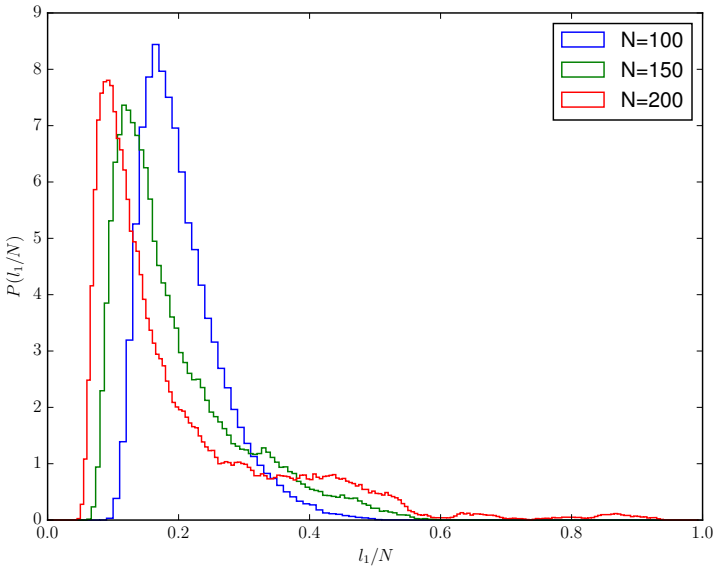

Figure 5.10: Histograms of $P(s/N)$ for cis sub-chain vs trans sub-chain (see Fig 5.9). Different curves correspond to different N values (see legend)

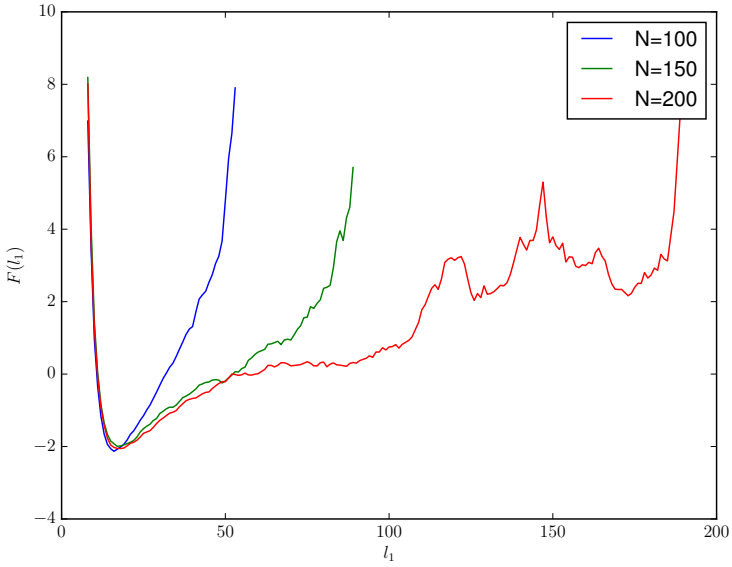

Figure 5.11: The profile of the free energy $F(s, N)$.Different curves correspond to different N values (see legend)

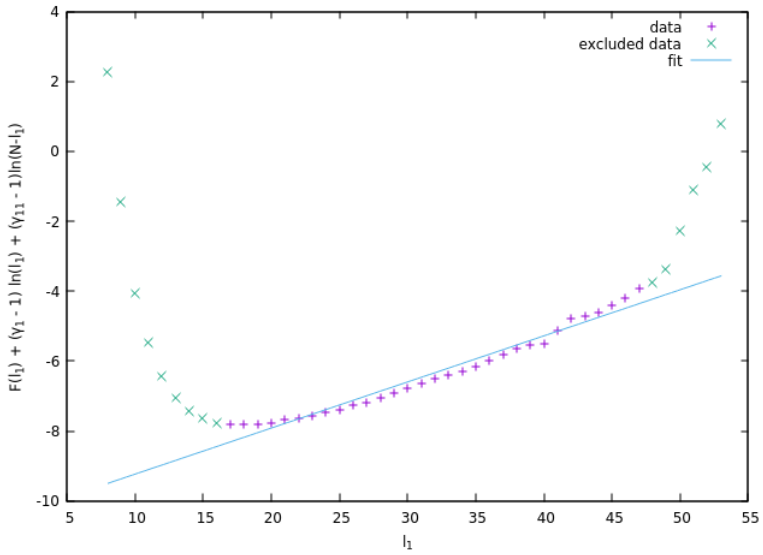

Figure 5.12: Plot of $F(N,s)+(\gamma_{11}-1)\ln s+(\gamma'_{11}-1)\ln(N-s)$ for $N=100$. The straight line represent the linear fit, the value of its angular coefficient is the difference of chemical potential $\Delta\kappa$.

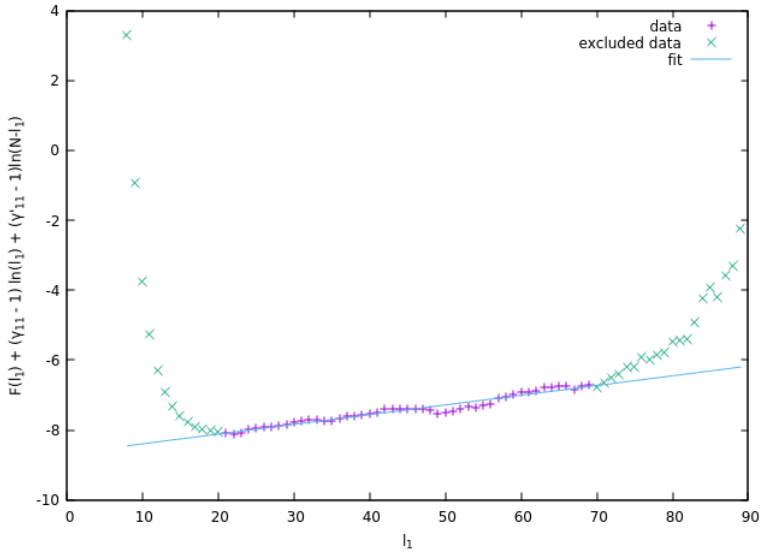

Figure 5.13: Plot of $F(N,s)+(\gamma_{11}-1)\ln s+(\gamma'_{11}-1)\ln(N-s)$ for $N=150$. The straight line represent the linear fit, the value of its angular coefficient is the difference of chemical potential $\Delta\kappa$.

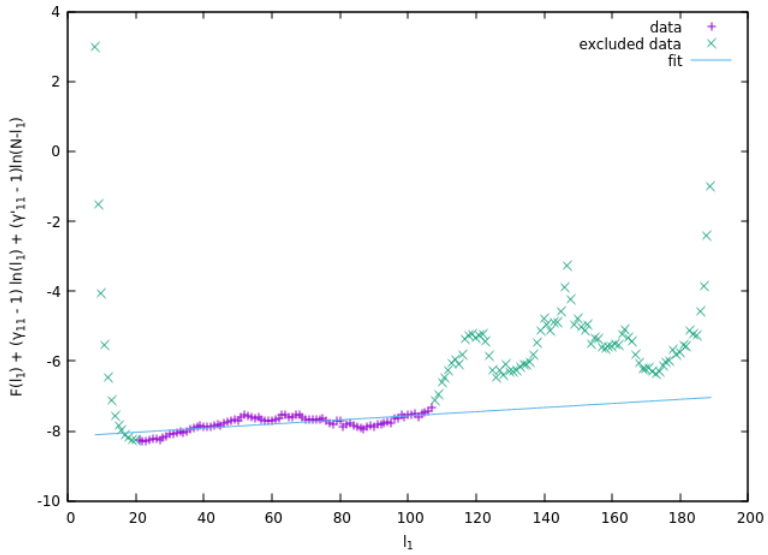

Figure 5.14: Plot of $F(N,s)+(\gamma_{11}-1)\ln s+(\gamma'_{11}-1)\ln(N-s)$ for $N=200$. The straight line represent the linear fit, the value of its angular coefficient is the difference of chemical potential $\Delta\kappa$.

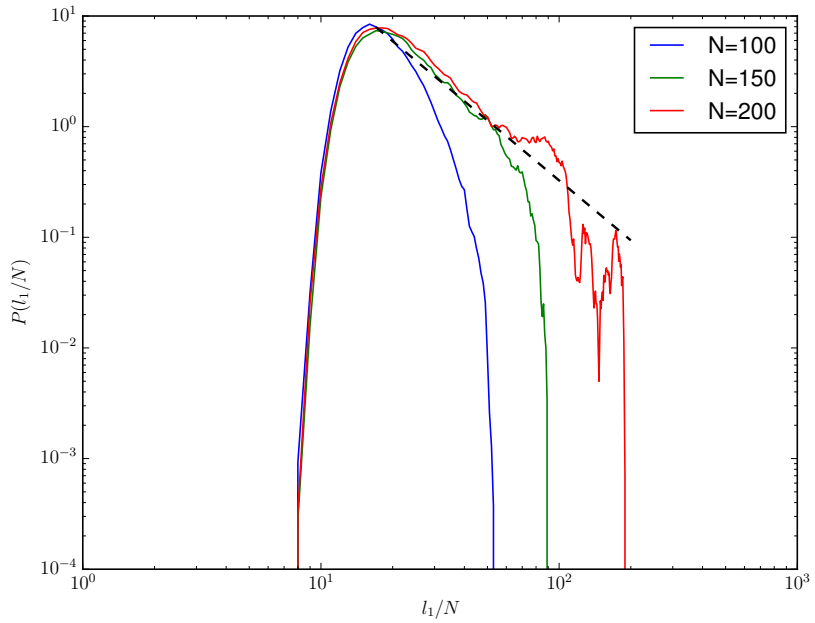

Figure 5.15: Log-log plot of $P(s)$. The dashed line represents a power law $s^{-1.75}$.

5.4 Polymer with a knot 4_1

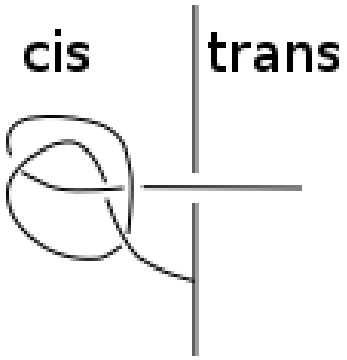

Figure 5.16: In figure there is a sketch showing the main topological features of the polymer: in the trans region the sub chain has one end attached to the wall, one fixed at the pore and has a knot 4_1, while in the cis region the sub chain has one end fixed at the pore and the other is free to move.

We consider a similar case to the one depicted in section 5.2, but we have tied a figure eight-knot: a sketch of the topology studied is represented in Fig 5.16.
We have sampled the PDF of s/N (see Fig. 5.17), the histograms have a different shape respect to the previous cases. The PDF, according to the theory, should resemble the one we have seen in section 5.3, the only difference should be only in the entropic exponent of the cis sub-chain. The exact entropic exponents are γ'_{11} and γ_1 respectively for the cis and the trans sub chain (for the configuration treated in section 5.2 they are γ_{11} and γ_1).
Due to the size of the knot in the cis region, the dominant configurations are the one with short trans sub chain (small $N - s$). But as N increase (see Fig 5.18) the peak shift to smaller value of s/N, in fact for very large N the behaviour should be similar to the first case we have treated.
This behaviour is due to the finite size corrections to the scaling laws and to the free energy: the presence of a knot strongly influences the shape of the free energy (see Fig 5.18). Differently from the previous case these corrections are not negligible at any N taken in consideration and the expression Eq. (5.2) for the free energy employed before is not applicable in this case.

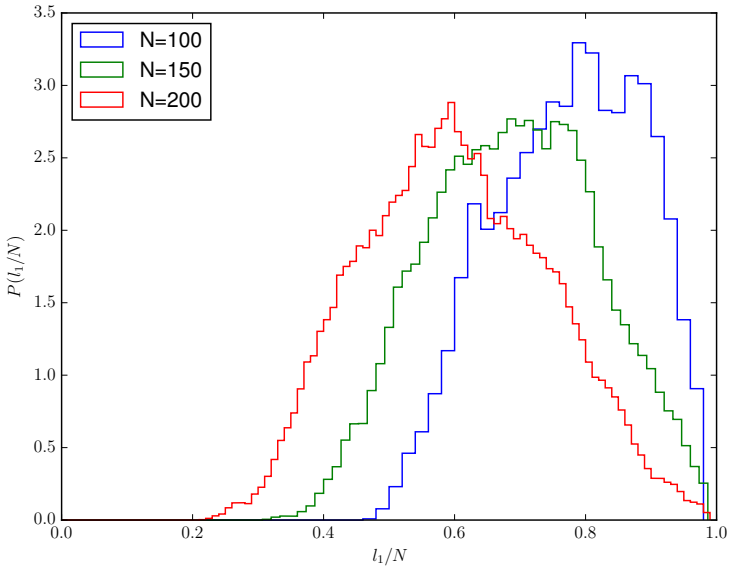

Figure 5.17: Histograms of $P(s/N)$ for cis sub-chain vs trans sub-chain (see Fig 5.16). Different curves correspond to different N values (see legend)

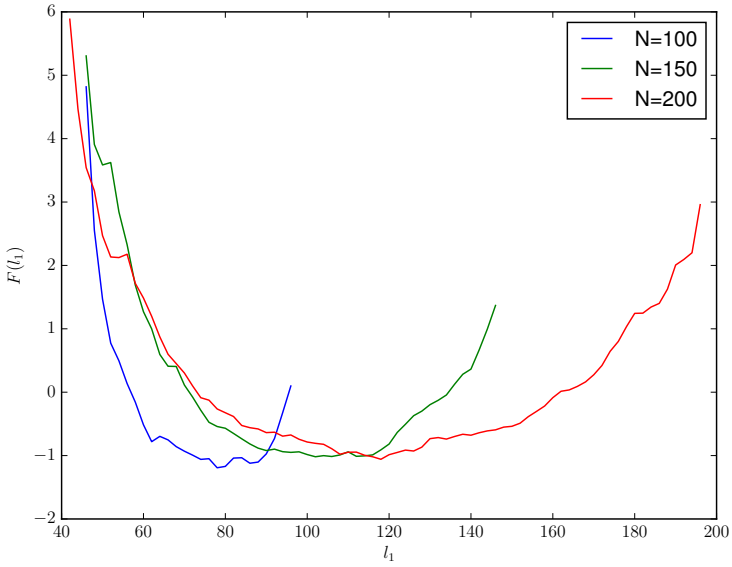

Figure 5.18: The profile of the free energy $F(s)$. Different curves correspond to different N values (see legend)

5.5 Polymer with a knot $3\#4$

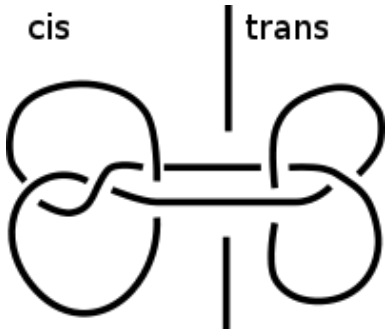

Figure 5.19: In figure there is a sketch showing the main topological features of the polymer: a ring polymer with a knot 4_1 tied in the cis region and a knot 3_1 tied in the trans region.

We consider the case of a translocation of a ring polymer with two knots (see Fig 5.19): a figure eight knot in the cis region and a trefoil knot in the trans region.
We assume that the two subsystem have same chemical potential, in fact it is believed that for self-avoiding polygons on a lattice $\mu_0 = \mu_3 = \mu_4$ (see Chapter 3), and we suppose that this relation it is still valid outside the lattice.
The PDF of s/N we have sampled does not present the bimodal shape. The distributions reported in Fig.5.20 show that the length of the loops keep fluctuating very broadly for increasing N.
The minimal length of the knot with four crossing is greater than the other: the effect in this case are not found in neither the subdominant nor the dominant term, it provides corrections to the scaling. Since the entropic exponents for the two sub chains are the same (γ'_{11}) the PDF should be symmetric respect $s/N = 1/2$, but the 4-crossing knot, being bigger, tends to shift the center of the distribution. Remarkably, the canonical average $\langle s/N \rangle_N$ follows an empirical law [3]:

$$\langle s/N \rangle_N = \frac{n_{c1}}{n_{c1} + n_{c2}} \tag{5.7}$$

where n_c is the number of crossing of the knot. In this case the loop with the 4_1 knot obtains on average a fraction of the chain length equal to $4/7 \approx 0.56$. As the number of the monomer grows the knot should be weakly localized and so in the thermodynamic limit the distribution tend to the one in which the knot are the same.

Due to the strong finite size corrections, we can't use the asymptotic form of the free energy used before and the profile of the free energy (see Fig 5.21) is very different from the one we expect for large N.

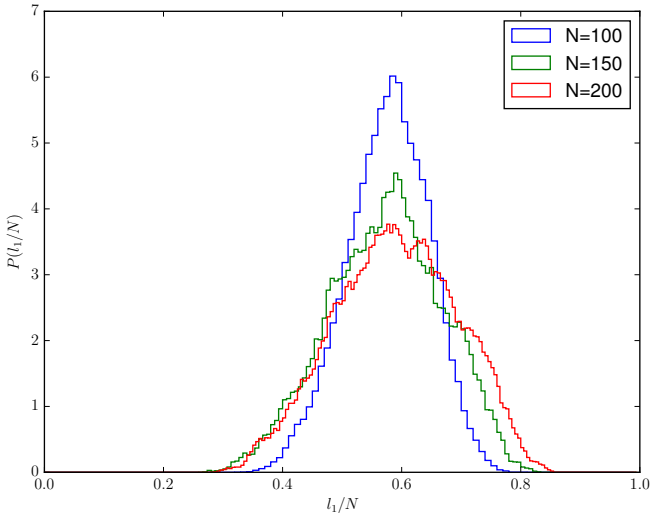

Figure 5.20: Histograms of $P(s/N)$ for 4_1 vs 3_1 (see Fig 5.19). Different curves correspond to different N values (see legend)

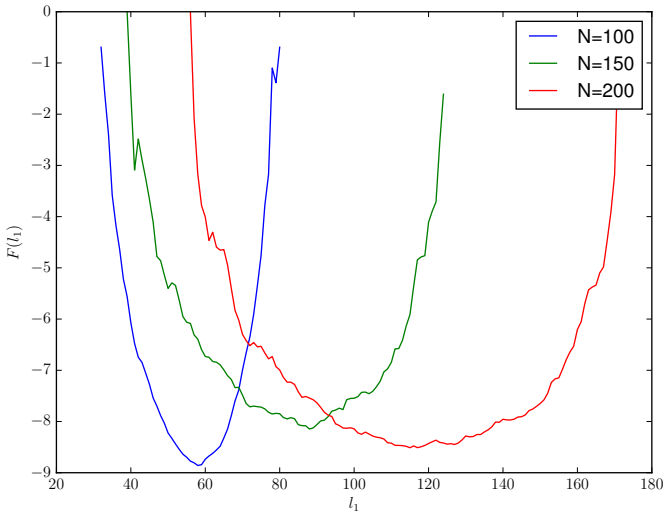

Figure 5.21: The profile of the free energy $F(s)$. Different curves correspond to different N values (see legend)

Chapter 6

Conclusion

The aim of this thesis was to explore the equilibrium and dynamical properties of polymers with a given topology translocating through a pore.
More precisely we simulated four systems with different topologies in which the polymer of different length N was translocating through a membrane pore and we tried to verify if the results based on the theory were compatible to the numerical data we found. We will refer to the cases studied using the following nomenclature: Case A (see Fig 5.2), Case B (see Fig 5.9), Case C (see Fig 5.16), Case D (see Fig 5.19).

For the first two topologies, case A and B, the results are consistent with the theory. Even if we couldn't completely neglect finite size corrections, the numerical data showed that the two systems follow quite well the scaling laws. The data was sufficient to estimate the entropic exponent γ_{11}, its value was very similar in both cases and compatible to the value we found in literature. We also estimated the difference of chemical potential $\Delta\kappa$ between the cis and trans region. In case A we obtained similar values for every N as we expected. In case B the value of $\Delta\kappa$ decreased for increasing N. The corrections to scaling were greater than the ones of case B, due to the presence of a knot, but they became negligible for large N, in fact $\Delta\kappa$ approached the predicted value ($\Delta\kappa_{exp} = 0$) as N grows.

The third topology, used in the case C, was quite troublesome. The presence of knots gives rise to strong corrections to scaling and we didn't observe its asymptotic behaviour, in order to do so we should use polymers with larger N. In the case D, as in the previous one, we had to consider strong corrections to scaling, due to the presence of two knots (one in the cis and one in the trans region), so we didn't observe the asymptotic behaviour. However, the results were consistent with the numerical ones obtained for a similar

problem studied on lattice [3].

This work could be improved in different ways. The MD simulations are computationally heavier than the Monte Carlo methods on a lattice model, so we could perform only simulations of polymers with a length up to $N = 200$ monomers. In order to simulate systems with a larger N we should use more powerful computing resources. For large N we should able to see better the asymptotic behaviour of the system. Furthermore, we can expand the work by considering other topologies: we could run simulations with other knot types in order to have more insights about the corrections to the scaling due to topology and their dependence on the knots type.

Bibliography

[1] M Baiesi, E Orlandini, and A L Stella. The entropic cost to tie a knot. *Journal of Statistical Mechanics: Theory and Experiment*, 2010(06):P06012, 2010.

[2] Marco Baiesi. *Geometry, Topology and Conformational Transitions in Double Stranded Heteropolymer*. University of Padua, 2002.

[3] Marco Baiesi, Enzo Orlandini, and Attilio L. Stella. Knotted globular ring polymers: How topology affects statistics and thermodynamics. *Macromolecules*, 47(23):8466–8476, 2014.

[4] Monica Iulia Bulacu. *Molecular dynamics studies of entangled polymer chains*. University Library of Groningen, 2008.

[5] Pierre-Gilles De Gennes. *Scaling concepts in polymer physics*. Cornell university press, 1979.

[6] K. De'Bell and Turab Lookman. Surface phase transitions in polymer systems. *Rev. Mod. Phys.*, 65:87–113, Jan 1993.

[7] Tetsuo Deguchi and Kyoichi Tsurusaki. Universality of random knotting. *Phys. Rev. E*, 55:6245–6248, May 1997.

[8] Jacques DesCloizeaux and Gérard Jannink. *Polymers in solution*. Clarendon Press Oxford, 1990.

[9] Masao Doi and Sam F Edwards. *The theory of polymer dynamics*, volume 73. oxford university press, 1988.

[10] Bertrand Duplantier. Polymer network of fixed topology: renormalization, exact critical exponent γ in two dimensions, and $d = 4 - \epsilon$. *Phys. Rev. Lett.*, 57:941–944, Aug 1986.

[11] J M Hammersley, G M Torrie, and S G Whittington. Self-avoiding walks interacting with a surface. *Journal of Physics A: Mathematical and General*, 15(2):539, 1982.

[12] CY Kong and M Muthukumar. Polymer translocation through a nanopore. ii. excluded volume effect. *The Journal of chemical physics*, 120(7):3460–3466, 2004.

[13] Marc Lackenby. The crossing number of composite knots. *Journal of Topology*, 2(4):747–768, 2009.

[14] B. Marcone, E. Orlandini, A. L. Stella, and F. Zonta. Size of knots in ring polymers. *Phys. Rev. E*, 75:041105, Apr 2007.

[15] Cristian Micheletti, Davide Marenduzzo, and Enzo Orlandini. Polymers with spatial or topological constraints: theoretical and computational results. *Physics Reports*, 504(1):1–73, 2011.

[16] Murugappan Muthukumar. Polymer translocation through a hole. *The Journal of Chemical Physics*, 111(22):10371–10374, 1999.

[17] Gordon Slade (auth.) Neal Madras. *The Self-Avoiding Walk*. Modern Birkhäuser Classics. Birkhäuser Basel, 1 edition, 2013.

[18] Christopher J Rasmussen, Aleksey Vishnyakov, and Alexander V Neimark. Translocation dynamics of freely jointed lennard-jones chains into adsorbing pores. *The Journal of chemical physics*, 137(14):144903, 2012.

[19] Michael Rubinstein. Polymer physics—the ugly duckling story: Will polymer physics ever become a part of "proper" physics? *Journal of Polymer Science Part B: Polymer Physics*, 48(24):2548–2551, 2010.

[20] Carlo Vanderzande. *Lattice models of polymers*, volume 11. Cambridge University Press, 1998.

[21] Hiromi Yamakawa. *Modern theory of polymer solutions*. Harper & Row, 1971.